Steady-state creep of discontinuous fibre composites

Pedersen, Ole Bøcker

Publication date:
1975

Document Version
Publisher's PDF, also known as Version of record

Risø Report No. 329

Risø Report No. 329

Danish Atomic Energy Commission

Research Establishment Risø

Steady-State Creep of Discontinuous Fibre Composites

by Ole Bøcker Pedersen

July 1975

Sales distributors: Jul. Gjellerup, 87, Sølvgade, DK-1307 Copenhagen K, Denmark

Available on exchange from: Library, Danish Atomic Energy Commission, Risø, DK-4000 Roskilde, Denmark

INIS Descriptors:

COMPOSITE MATERIALS
COPPER
CREEP
FIBERS
MATHEMATICAL MODELS
REINFORCED MATERIALS
STRESS ANALYSIS
TUNGSTEN

UDC 621.763 : 539.434

July 1975 Risø Report No. 329

Steady-State Creep of Discontinuous Fibre Composites

by

Ole Bøcker Pedersen

Danish Atomic Energy Commission
Research Establishment Risø
Metallurgy Department

and

Technical University of Denmark
Department of Structural Properties of Materials

Abstract

A review is given of the relevant literature on creep of composites, including a presentation of existing models for the steady-state creep of composites containing aligned discontinuous fibres where creep of the matrix and fibres is assumed to follow a power law. A model is suggested for predicting the composite creep law from a matrix creep law given in a general form, in the case where the fibres do not creep. The composite creep law predicted by this model is compared with those predicted by previous models, when these are extended to comprise a general matrix creep law. Experimentally, pure copper and composites consisting of aligned discontinuous tungsten fibres in a copper matrix were creep tested at a temperature of 500°C. The results indicate a relatively low stress sensitivity of the steady-state creep-rate for pure copper and a relatively high stress sensitivity for the composites. This may be explained by the creep models based upon a general matrix creep law. A quantitative prediction shows promising agreement with the present experimental results.

ISBN 87 550 0350 8

PREFACE

The present dissertation is submitted to The Technical University of Denmark in partial fulfilment of the requirements for the degree of licentiatus technices (lic. techn.).

The dissertation describes research carried out in the period from 15 August 1972 to 1 April 1975 under the supervision of Professor R. M. J. Cotterill, Department of Structural Properties of Materials, The Technical University of Denmark, and lic. techn. H. Lilholt, Danish Atomic Energy Commission, Research Establishment Risø, Metallurgy Department.

I would like to thank Professor Cotterill for allowing me to study in his department and for his interest and encouragement. I should also like to thank Dr. techn. N. Hansen, head of the Metallurgy Department, Risø, for providing research facilities in the Metallurgy Department.

I am indebted to several members of the Metallurgy Department. Lic. techn. H. Lilholt suggested the general course of this research, and my thanks are due to him and to lic. techn. J. B. Bilde-Sørensen for fruitful collaboration and stimulating criticism. Furthermore, I thank J. Kjøller, J. Larsen, P. Nielsen, O. Olsen, and H. Nilsson for excellent technical assistance.

Finally, I wish to thank the other lic. techn. students and the members of the Department of Structural Properties of Materials for their kindness and pleasant company, which I have greatly appreciated.

The financial support of the Danish Atomic Energy Commission in the period from 15 August 1972 to 1 April 1975 is gratefully acknowledged.

O. Bøcker Pedersen

CONTENTS

1. INTRODUCTION

Two-phase materials are generally intended for high-temperature structural applications, and a basic understanding of their creep properties is thus of great practical as well as fundamental interest. The present work deals with the uniaxial steady-state creep of composites containing discontinuous fibres aligned in the loading direction. The primary aim has been to elucidate the relation between creep properties of the composite, creep properties of the components, and structural parameters including fibre content, fibre length and fibre spacing.

At the time that this study was started Kelly and Tyson (1966) had investigated the creep of silver containing discontinuous tungsten fibres under conditions where the creep of the fibres could be neglected, while Kelly and Street (1972a) had studied the creep of lead containing discontinuous creeping phosphor bronze fibres.

Several models (Mileiko 1970 ; McLean 1972 ; and Kelly and Street 1972b) had also been put forward. These models led to essentially identical predictions of the composite creep strength (Lilholt 1972);but their agreement with experiments was not completely satisfactory. It therefore appeared that in order to extend the understanding of creep of fibre composites, refinement of theory was needed as well as more experimental data.

This dissertation contains a general description of the creep properties of crystalline solids (section 2), followed by an outline of the relevant studies of the creep of fibre composites (section 3). The present theoretical (section 4) and experimental (sections 5 and 6) investigation of the creep of fibre composites is then described and discussed (section 7). Most of the present work has been published elsewhere (Bøcker Pedersen 1974a; 1974b; 1975 ; and Bilde-Sørensen, Bøcker Pedersen, and Lilholt 1975).

2. GENERAL ASPECTS OF CREEP

In a conventional creep test of a solid a constant uniaxial stress/load is applied and deformation along the stress axis is recorded as a function of time at constant temperature. The resulting time-deformation curve, which is traditionally called the creep curve, depends mainly upon stress and temperature. In the region of high-temperature creep, i.e. at temperatures and stresses exceeding approximately $0.4\ T_m$ and $10^{-5}\ G$, respectively, the creep curve for polycrystalline solids normally displays three regions: the primary region characterized by a time-dependent strain-rate, the secondary region characterized by a constant strain-rate, and the tertiary region

characterized by an increasing strain-rate and terminated by rupture.

The study of creep of fibre composites is in this report confined to the secondary region, which is traditionally called the steady-state region.

2.1. Creep Law of Crystalline Solids

The uniaxial applied stress as a function of the resulting creep-rate in the steady-state region,

$$\sigma = f(\dot{\epsilon}) , \qquad (1)$$

is often referred to as the creep law. A large number of creep data (Sherby and Burke 1967 ; Bird, Mukherjee, and Dorn 1969 ; Ashby 1972) indicate that the creep law for pure crystalline solids can be fairly generally represented by a diagram of the type shown in fig. 1.

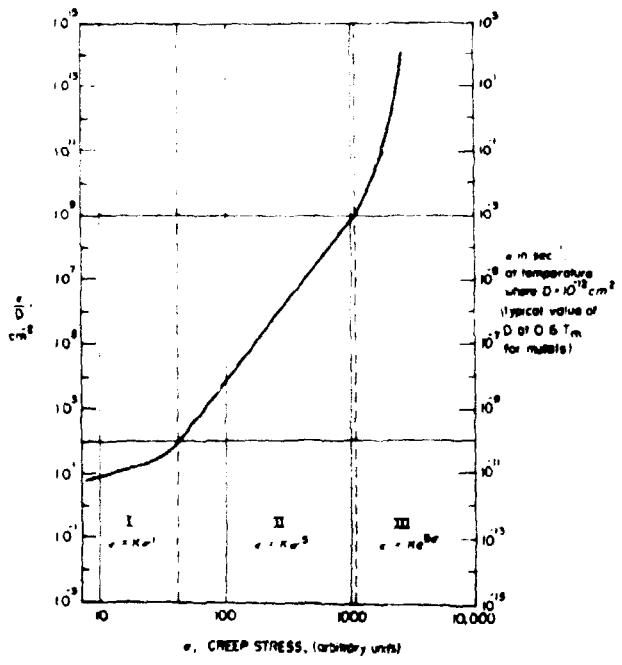

Fig. 1. Influence of stress on the diffusion-compensated steady state creep rate for a typical pure polycrystalline metal. It is believed that range I is due to a diffusional creep process whereas range II is controlled by dislocation climb involving an equilibrium vacancy concentration. Range III involves dislocation climb creep under conditions where the vacancy concentration is greater than the thermal equilibrium number (Sherby and Burke, 1967).

In this diagram the diffusion-compensated steady-state creep-rate, $\dot{\varepsilon}/D$, is used, since the steady-state creep-rate is normally proportional to the diffusion coefficient

$$D = D_o \exp\left(-\frac{E + P\Omega}{kT}\right). \qquad (2)$$

The diagram therefore also indicates the effect of temperature, T, and hydrostatic stress, P, on $\dot{\varepsilon}$ via the effect of these parameters on self-diffusion.

The hydrostatic term,

$$\exp\left(-\frac{P\Omega}{kT}\right),$$

which agrees reasonably well with experiments at relatively high hydrostatic pressure (McCormick and Ruoff 1970), is usually close to unity and hence fairly insignificant. It may be mentioned, however, that recent work (Needham, and Greenwood 1975) has indicated that the decrease of $\dot{\varepsilon}$ caused by a relatively low hydrostatic pressure is too large to be attributed solely to the effect of pressure on diffusion.

Fig. 1 represents the typical stress dependence of the steady-state creep-rate, but there are exceptions to the rule. Ardell and Sherby (1967) found that the stress sensitivity, $\partial \log\dot{\varepsilon}/\partial\log\sigma$, of alpha zirconium decreases as the applied stress is increased. Similar behaviour is found for polycrystalline Fe_2O_3 at low stresses, but experiments over a wide range of stress show that the $\log\dot{\varepsilon}$-$\log\sigma$ curve for Fe_2O_3 is in fact "S" shaped (Crouch 1972, and Pascoe 1974) and that the highest stress sensitives occur at high stresses. Hay and Pascoe (1974) recently described the creep of Fe_2O_3 at low stresses by a model involving interdependent deformation mechanisms. Mathematically, their model bears some resemblance to the simple theory for creep of composites containing continuous fibres (Mc Danels, Signorelli, and Weeton 1967, and Street 1971).

2.2. Creep in Shear Under Multiaxial Stress

Equation 1 is a tensile relation, in the sense that it relates the tensile stress to the tensile creep-rate. However, the matrix in a creeping fibre composite is expected to deform primarily in shear parallel to the fibres. In the present study it is therefore necessary to be able to convert eq.1 into a shear

relation, i.e. a relation between a shear stress and the corresponding shear creep-rate. Furthermore, the stress system in a creeping composite cannot be expected to be a simple uniaxial stress. It is therefore also important to understand the creep behaviour of solids subjected to multiaxial stress. These questions will be considered for a plastic continuum in the present section.

2.2.1. Multiaxial State of Stress

In order to describe the steady-state creep behaviour of a solid subjected to multiaxial stress a relation which is more general than the creep law for uniaxial stress is needed. This relation should involve the stress tensor, σ_{ij}, and the creep-rate tensor, $\dot{\epsilon}_{ij}$, referred to a set of cartesian axes, $0\text{-}x_i$. Odquist (1966) has derived such a relation for an incompressible and plastically isotropic continuum which obeys a power law

$$\sigma = \sigma_o \left(\frac{\dot{\epsilon}}{\dot{\epsilon}_o}\right)^{1/n} = f_p(\dot{\epsilon}) , \tag{3}$$

when it is subjected to uniaxial stress. Odquist further made the hypotheses that the principal axes of σ_{ij} and $\dot{\epsilon}_{ij}$ are coincident and that $\dot{\epsilon}_{ij}$ is not influenced by a hydrostatic stress. His equation is

$$\dot{\epsilon}_{ij} = \frac{3}{2}\dot{\epsilon}_o \left(\frac{\sigma_e}{\sigma_o}\right)^{n-1} \frac{s_{ij}}{\sigma_o} , \tag{4}$$

where s_{ij} is the stress deviator,

$$s_{ij} = \sigma_{ij} - \frac{1}{3}\delta_{ij}\sigma_{kk} ,$$

δ_{ij} is the Kronecker symbol,

$$\delta_{ij} = \begin{cases} 1 & \text{if} \quad i = j \\ 0 & \text{if} \quad i \neq j \end{cases} ,$$

and σ_e is the effective stress,

$$\sigma_e^2 = \frac{3}{2} s_{ij} s_{ij} .$$

In these expressions summation over the values 1, 2 and 3 is implied with respect to any index occurring twice in the same term.

It is convenient to introduce the two sets of reference axes shown in fig. 2. The $0\text{-}x_i^P$ axes are the principal (P) axes of the stress tensor. Referred to these axes the stress tensor takes the form

$$\sigma_{ij}^P = \begin{pmatrix} \sigma_1 & 0 & 0 \\ 0 & \sigma_2 & 0 \\ 0 & 0 & \sigma_3 \end{pmatrix}, \tag{5}$$

where the diagonal elements are the principal stresses.

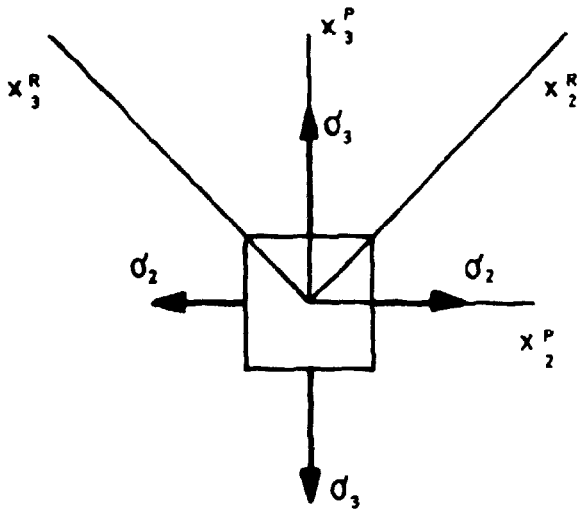

Fig. 2. The stress tensor referred to the principal axes, $0\text{-}x_i^P$. The axes, $0\text{-}x_i^R$, are rotated through 45° about the $0\text{-}x_1^P$ axis, which is directed out of the plane of the paper.

The second set of axes, $0\text{-}x_i^R$, is rotated (R) through 45° about the $0\text{-}x_1^P$ axis. The stress tensor, σ_{ij}^R, referred to these axes can be obtained from σ_{ij}^P using the general transformation rule for tensors (see e.g. Jeffreys 1963)

$$\sigma_{ij}^R = a_{ik}\, a_{jl}\, \sigma_{kl}^P$$

with

$$a_{ij} = \begin{pmatrix} 1 & 0 & 0 \\ 0 & \frac{\sqrt{2}}{2} & \frac{\sqrt{2}}{2} \\ 0 & -\frac{\sqrt{2}}{2} & \frac{\sqrt{2}}{2} \end{pmatrix} .$$

Carrying out the transformation one obtains

$$\sigma^R_{ij} = \begin{pmatrix} \sigma_1 & 0 & 0 \\ 0 & \frac{1}{2}(\sigma_2 + \sigma_3) & \frac{1}{2}(\sigma_3 - \sigma_2) \\ 0 & \frac{1}{2}(\sigma_3 - \sigma_2) & \frac{1}{2}(\sigma_2 + \sigma_3) \end{pmatrix} . \qquad (6)$$

In the following text an "R" or a "P" attached to a tensor is meant to indicate that the tensor is referred to $0\text{-}x^R_i$ or $0\text{-}x^P_i$, respectively.

I shall now consider a special multiaxial stress system, and as an illustrative and simple case I shall take the system for which $\sigma_1 = \sigma_2 = \sigma_T < \sigma_3 = \sigma_L$. The matrices (5) and (6) can in this case be written

$$\sigma^P_{ij} = \begin{pmatrix} \sigma_T & 0 & 0 \\ 0 & \sigma_T & 0 \\ 0 & 0 & \sigma_L \end{pmatrix} \text{ and } \sigma^R_{ij} = \begin{pmatrix} \sigma_T & 0 & 0 \\ 0 & \frac{1}{2}(\sigma_L + \sigma_T) & \frac{1}{2}(\sigma_L - \sigma_T) \\ 0 & \frac{1}{2}(\sigma_L - \sigma_T) & \frac{1}{2}(\sigma_L + \sigma_T) \end{pmatrix} .$$

According to eq. 4 this stress system causes a pure extension of the solid described by the matrices

$$\dot{\epsilon}^P_{ij} = \begin{pmatrix} -\frac{1}{2}\dot{\epsilon} & 0 & 0 \\ 0 & -\frac{1}{2}\dot{\epsilon} & 0 \\ 0 & 0 & \dot{\epsilon} \end{pmatrix} \text{ and } \dot{\epsilon}^R_{ij} = \begin{pmatrix} -\frac{1}{2}\dot{\epsilon} & 0 & 0 \\ 0 & \frac{1}{4}\dot{\epsilon} & \frac{3}{4}\dot{\epsilon} \\ 0 & \frac{3}{4}\dot{\epsilon} & \frac{1}{4}\dot{\epsilon} \end{pmatrix} ,$$

where

$$\dot{\varepsilon} = \dot{\varepsilon}_o \left(\frac{\sigma_L - \sigma_T}{\sigma_o}\right)^n . \qquad (7)$$

In a composite containing non-creeping aligned fibres the transverse contraction of the creeping matrix will be resisted by the fibres, which exert a transverse stress on the matrix in addition to the longitudinal stress. The stress system in the composite is therefore of the type considered in this section. Eq. 7 illustrates the effect of the transverse stress, by showing that the quantity causing the deformation is $\sigma_L - \sigma_T$ rather than just σ_L. An unlimitedly high value of σ_L is therefore in principle possible, at a given $\dot{\varepsilon}$, provided it is off-set by an appropriate value of σ_T.

2.2.2. Shear Relations

In order to obtain a shear relation corresponding to the special situation considered in section 2.2.1., I shall look at the stress- and creep-rate resolved along planes at 45° to the 0-x_3^P axis, i.e. resolved along, say 0-x_2^R. The shear creep-rate component is given by

$$\frac{\dot{\gamma}}{2} = \dot{\varepsilon}^R_{32} = \frac{3}{4}\dot{\varepsilon}$$

and the shear stress by

$$\tau = \sigma^R_{32} = \frac{1}{2}(\sigma_L - \sigma_T) .$$

In combination with eq. 7 these equations give the shear relation

$$2\tau = \sigma_o \left(\frac{2\dot{\gamma}}{3\varepsilon_o}\right)^{1/n} = f_P\left(\frac{2}{3}\dot{\gamma}\right) . \qquad (8)$$

As a special case eq. 8 applies to the maximum shear values in the ordinary tensile creep test (where $\sigma_T = 0$).

Kelly and Street (1972b), in their model for creep of fibre composites, use eq. 8 as the shear relation. McLean (1972), however, refers to the slightly different relation

$$2\tau = \sigma_o \left(\frac{\dot{\gamma}}{2\varepsilon_o}\right)^{1/n} = f_P\left(\frac{1}{2}\dot{\gamma}\right) . \qquad (9)$$

Equation 9 would apply if there was no transverse contraction in, for instance, the $0\text{-}x_1^P$ direction. Although this situation is not included in eq. 4, which represents the isotropic case, it is, of course, a possibility for anisotropic materials.

Shear relations for stress systems other than the one corresponding to the normal tensile creep test can also be derived. An example is

$$\sqrt{3}\tau = \sigma_o \left(\frac{\gamma}{\sqrt{3}\,\dot{\varepsilon}_o}\right)^{1/n} = f_P\left(\frac{\dot{\gamma}}{\sqrt{3}}\right), \qquad (10)$$

which is obtained from eq. 4 by inserting the stress tensor for pure shear (i.e. $\sigma_1 = 0$ and $-\sigma_2 = \sigma_3 = \tau$) and proceeding along the lines which, for pure extension, led to eq. 8.

The shear relations given by eqs. 8-10 do not differ greatly and in the following I shall consistently use eq. 8 as the shear relation for a power creep law, f_P, even when presenting creep models which do not involve eq. 8 in their original form. I shall furthermore use the relation

$$2\tau = f\left(\frac{2}{3}\dot{\gamma}\right) \qquad (11)$$

as the shear relation for a creep law, f, which may be any continuous function. Equation 11 applies for the maximum shear values in a tensile creep test of an isotropic incompressible material in which the steady-state creep rate is uninfluenced by a superimposed hydrostatic stress.

3. REVIEW OF PREVIOUS WORK

There has been some interest in the creep properties of composites containing aligned continuous or discontinuous fibres. A review of the early literature is given by Kelly (1971) while Lilholt (1972) has reviewed the more recent studies of the steady-state creep of composites containing discontinuous fibres (deSilva 1968; Mileiko 1970; Kelly and Street 1972a and b; and McLean 1972).

In the literature it is often assumed that the creep properties of one component are uninfluenced by the presence of the other component. In metallic composites this assumption can be expected to be valid when the fibre spacing, Λ, exceeds roughly 10 μm, but at smaller fibre spacings there is experimental evidence suggesting that the fibres and matrix modify the mechanical properties of one another:

Measurements of the stress-strain curves of composites containing continuous fibres (Cheskis and Heckel 1968 ; Stuhrke 1968 ; Kelly and Lilholt 1969 ; and Garmong and Shepard 1971) demonstrate that very high longitudinal tensile stresses exist in the matrix at strains where the matrix is plastic but the fibres are still elastic. The fact that the matrix stresses decrease when the fibres yield suggests that they arise as a result of transverse stresses generated by a difference in the transverse contraction of fibres and matrix (Kelly and Lilholt 1969). In this interpretation the high matrix stresses are of course not due to a modification of the matrix creep properties as such; but rather to the change of behaviour associated with the occurrence of multiaxial stresses. However, the high matrix stresses could also be due to a genuine strain-hardening of the matrix. Lilholt (1973) discussed the influence of fibre spacing on the basis of geometrically necessary dislocations (Ashby 1971). He showed that the role played by the fibre spacing in a composite has some similarity to the role played by the grain size in a polycrystal. Kelly (1971a; 1971b; 1972a; and 1973a) discussed the relationship between dispersion strengthening and fibre reinforcement. Finely spaced fibres, $\Lambda \sim 10\,\mu m$, should strengthen the matrix in a way similar to that known from dispersion strengthening.

The following subsections give a brief description of the literature relevant to the present work . In this literature it is assumed that the creep properties of one component are not modified by the presence of the other component. The creep theories are presented in a slightly simplified form, since the emphasis is on physical ideas rather than mathematical detail.

3.1. Kelly and Tyson

Kelly and Tyson (1966) consider theoretically the distribution of longitudinal tensile stress, $\sigma_f(z)$, in a discontinuous non-creeping fibre in a creeping composite. The stress is transferred to the fibre by the interface shear stress, τ_i, according to the general stress balance

$$\frac{d\sigma_f}{dz} = -\frac{4\tau_i}{d} \quad . \tag{12}$$

When the load is applied to the composite, Kelly and Tyson suppose that the matrix in the vicinity of the fibre ends is strained beyond its yield strain. At the fibre ends τ_i therefore equals the yield stress corresponding to the high strain-rate following the application of the load. The corresponding σ_f-distribution is represented by curve a in fig. 3.

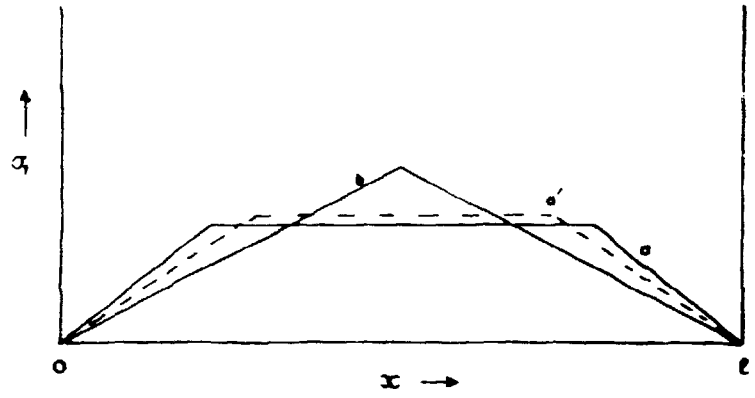

Fig. 3. Schematic variation of tensile stress with distance along a fibre of length l (Kelly and Tyson, 1966).

Kelly and Tyson ignore the tensile load carried by the matrix, and express the creep strength by

$$\sigma_c = V_f \bar{\sigma}_f , \tag{13}$$

where the average tensile stress in the fibre, $\bar{\sigma}_f$, is defined as

$$\bar{\sigma}_f = \frac{2}{l} \int_0^{l/2} \sigma_f dz . \tag{14}$$

During the initial part of the creep test the interface shear stress will gradually decrease by stress relaxation. This replaces the initial distribution (curve a) by a succession of distributions, represented by curve a', which must all satisfy eq. 13 with a constant value for σ_c. When steady-state creep finally prevails Kelly and Street expect the distribution to look like the approximately linear curve b. The slope of this curve, according to eq. 12, represents the smallest value of τ_i consistent with eq. 13. In order to maintain this distribution the matrix must creep in shear parallel to the fibre.

By introducing a constant value of τ_i into eqs. 12, 13 and 14, and ignoring the end stress on the fibre, Kelly and Tyson find that

$$\sigma_c = \tau_i \rho V_f . \tag{15}$$

Equation 15 predicts that the creep strength should vary roughly proportionally with the fibre aspect ratio and the fibre volume fraction, in essential agreement with later more refined analyses. However, since eq. 15 does not explicitly involve $\dot{\epsilon}_c$, it is, of course, not a complete description of the steady-state creep of the composite.

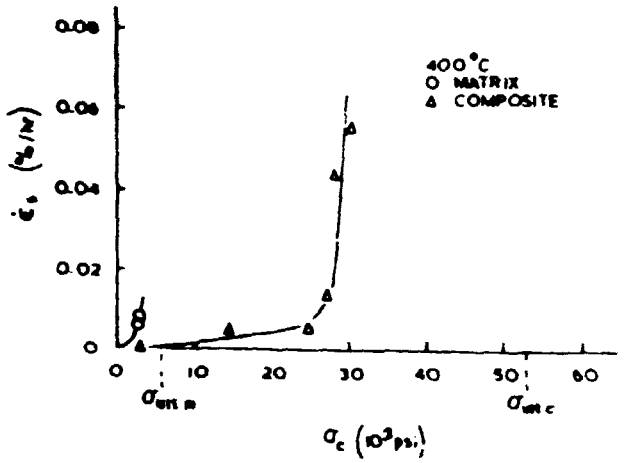

Fig. 4. Variation of minimum creep rate with stress on a composite compared with the rate of creep of the matrix (Kelly and Tyson, 1966).

Experimentally, Kelly and Tyson investigated the creep of silver containing 40 vol.% tungsten fibres of aspect ratios 30 or 60 and diameter 200 μm. The composites were fabricated by liquid infiltration and creep tested in air at 400°C, 500°C and 600°C under constant loads sufficiently small that negligible creep occurred in the fibres. Creep data were also obtained for pure silver. The creep curves for the composites displayed well-developed regions of steady-state creep. Fig. 4 shows some of the results.

Kelly and Tyson found that the creep strength increased with increasing values of the fibre aspect ratio, in qualitative agreement with eq. 15; but the variation of σ_c with ρ observed in the experiments is less than expected on the basis of eq. 15. They finally observe that: "At any one temperature there is a transition which occurs with increasing stress, from a region of small stress dependence where the creep-rate varies as about the third power of the applied stress, to a region of very much higher stress dependence".

3.2. Mileiko

The simple version of Mileiko's (1970) model is a combination of unit elements consisting of two rigid plates attached to a slab of matrix, as shown in fig. 5a. The simplest combination of unit elements is obtained for symmetrical overlap (i.e. $l' = L/2$, see fig. 5b).

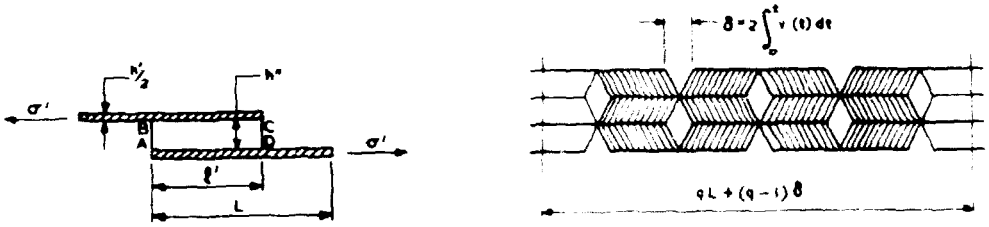

(a) (b)

Fig. 5. The creep model by Mileiko (1970).

The elongation of the model composite occurs by simple shear of the matrix slabs. As illustrated by fig. 5b this causes holes to open up at the ends of the plates. Similar holes are associated with the flow patterns in the models by Kelly and Street (1972b) and McLean (1972). Mileiko does not consider this to be important.

Mileiko calculates the rate of relative displacement, v, of the plates on the basis of the unit element shown in fig. 5a. However, this element experiences a net torque. It is therefore not in static equilibrium, and hence it cannot represent the construction shown in fig. 5b. I shall replace it by the modified element shown in fig. 6, in which the symbols are altered so as to conform to the notation used in the present text.

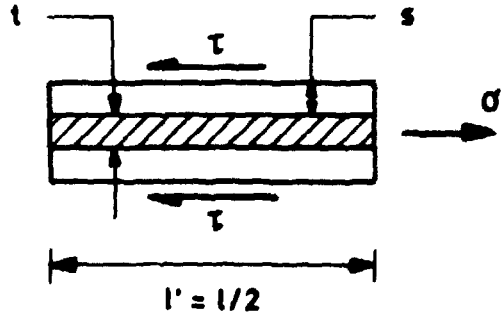

Fig. 6. Modified plate-like unit element.

The modified element represents the construction and is in static equilibrium when

$$\tau l = t\sigma . \qquad (16)$$

Mileiko assumes that the matrix creeps according to a power law and by introducing eq. 8 into eq. 16, the rate of relative displacement of adjacent plates can be written

$$v = s\dot{\gamma} = \frac{3}{2} s \dot{\varepsilon}_o \left(\frac{2t\sigma}{\sigma_o l}\right)^n . \tag{17}$$

The rate of elongation of the model composite (see fig. 5b) is expressed approximately as

$$\dot{\varepsilon}_c = \frac{2v}{l} . \tag{18}$$

In Mileiko's terminology the plates are referred to as "fibres". The fibre volume fraction is defined as

$$V_f = \frac{t}{t+s} \tag{19}$$

and the fibre aspect ratio as

$$\rho = \frac{l}{t} . \tag{20}$$

The tensile load supported by the matrix is taken to be negligible and the composite creep strength defined as

$$\sigma_c = V_f \sigma . \tag{21}$$

Combination of eqs. 17-21 yields

$$\sigma_c = c\, V_f \sigma_o \left(\frac{\dot{\varepsilon}_c}{\dot{\varepsilon}_o}\right)^{1/n} \rho^{1+1/n} \tag{22}$$

with

$$c = \frac{1}{2}\left(\frac{1}{3}\right)^{1/n} \left(\frac{V_f}{1 - V_f}\right)^{1/n} .$$

Mileiko extends his model to include hexagonally distributed fibres of hexagonal cross-section, and he allows the overlap, l', to have a random distribution between l' = 0 and l' = l. The difference between the strength predicted for random overlap and for symmetric overlap is a factor of roughly $2^{1-1/n}$. Mileiko also discusses the situation in which the fibre load is sufficiently great to produce fibre creep or fibre rupture.

3.3. Kelly and Street

The model by Kelly and Street (1972 b) refers to the general situation illustrated by fig. 7, where creep occurs in both fibres and matrix, and sliding takes place at the fibre/matrix interface.

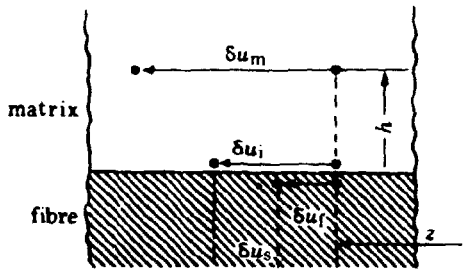

Fig. 7. Section of composite parallel to fibre axis showing the displacements during a time interval of a point in the matrix at a distance h from the interface δu_m, a point at the interface δu_i; and a point in the fibre δu_f (Kelly and Street 1972b).

I shall first present Kelly and Street's analysis of the case of non-creeping fibres and perfect interface bond. Then I shall describe how Kelly and Street extend their model to the situation in which the fibres experience creep.

In both cases Kelly and Street assume that the matrix is sheared at the rate of

$$\dot{\gamma} = \frac{\delta u_m - \delta u_i}{h\,\delta t} = \frac{\dot{u}_m - \dot{u}_i}{h}. \tag{23}$$

This equation involves holes at the fibre ends. However, Kelly and Street are especially concerned with the situation far from the fibre ends, and hence they do not consider this question.

When the fibres do not creep, i. e. $\delta u_f = 0$, and there is no interface sliding, i. e. $\delta u_s = 0$, then the rate of displacement relative to the fibre of a point in the matrix adjacent to the interface is zero

$$\dot{u}_i = \frac{\delta u_f + \delta u_s}{\delta t} = 0. \tag{24}$$

The rate of displacement relative to the fibre of a point in the matrix at a distance h from the interface is

$$\dot{u}_m = \dot{\epsilon}_c z. \tag{25}$$

Kelly and Street set h equal to half the minimum spacing between the surfaces of fibres arranged in a hexagonal pattern

$$h = \alpha d \tag{26}$$

where

$$\alpha = \frac{1}{2}\left[\left(\frac{2\sqrt{3}}{\pi} V_f\right)^{-1/2} - 1\right]$$

and by combining eqs. 23 - 26 they obtain

$$\dot{\gamma} = \frac{\dot{\epsilon}_c z}{\alpha d}. \tag{27}$$

Kelly and Street assume that the matrix creeps according to a power law. Taking eq. 8 as the shear relation and using eq. 27, they obtain the interface shear stress

$$\tau_i = \frac{1}{2}\left(\frac{2}{3\alpha}\right)^{1/n} \sigma_o \left(\frac{\dot{\epsilon}_c}{\dot{\epsilon}_o}\right)^{1/n} \left(\frac{|z|}{d}\right)^{1/n}. \tag{28}$$

For higher values of n the interface shear stress is, according to eq. 28, seen to be approximately independent of z. Equation 28 is therefore in essential agreement with the models by Kelly and Tyson (1966) and Mileiko (1970) that both involve a constant τ_i.

The distribution of longitudinal tensile stress in the fibre is found by combining eqs. 12 and 28 and integrating with respect to z, under the assumption that $\sigma_f = 0$ at $z = l/2$, the result is

$$\sigma_f = \frac{2n}{n+1}\left(\frac{2}{3\alpha}\right)^{1/n} \sigma_o \left(\frac{\dot{\epsilon}_c}{\dot{\epsilon}_o}\right)^{1/n} \left[\left(\frac{1}{2d}\right)^{\frac{n+1}{n}} - \left(\frac{|z|}{d}\right)^{\frac{n+1}{n}}\right]. \tag{29}$$

The average tensile stress in the fibre, $\bar{\sigma}_f$, is found by introducing eq. 29 into eq. 14

$$\bar{\sigma}_f = \frac{n}{2n+1}\left(\frac{1}{3\alpha}\right)^{1/n} \sigma_o \left(\frac{\dot{\epsilon}_c}{\dot{\epsilon}_o}\right)^{1/n} \rho^{1+1/n} \tag{30}$$

Kelly and Street define the composite creep strength as

$$\sigma_c = V_f \bar{\sigma}_f + V_m \bar{\sigma}_m \tag{31}$$

with

$$\bar{\sigma}_m = \sigma_o \left(\frac{\dot{\varepsilon}_c}{\dot{\varepsilon}_o}\right)^{1/n} = f_P(\dot{\varepsilon}_c) .$$

A contribution from the matrix is seen to be included via the additive term, $V_m \bar{\sigma}_m$. This term, however, is found by numerical calculations (Bilde-Sørensen, Bøcker Pedersen and Lilholt 1975) to contribute less than 20% when $\rho V_f \gtrsim 4$. When ρ is not too small the term can therefore be ignored and the composite creep strength be written

$$\sigma_c = c\, V_f \sigma_o \left(\frac{\dot{\varepsilon}_c}{\dot{\varepsilon}_o}\right)^{1/n} \rho^{1+1/n} \qquad (32)$$

with

$$c = \frac{n}{2n+1} \left(\frac{1}{3a}\right)^{1/n} .$$

In order to account for the situation in which the fibres themselves experience creep, Kelly and Street assume the model shown in fig. 8

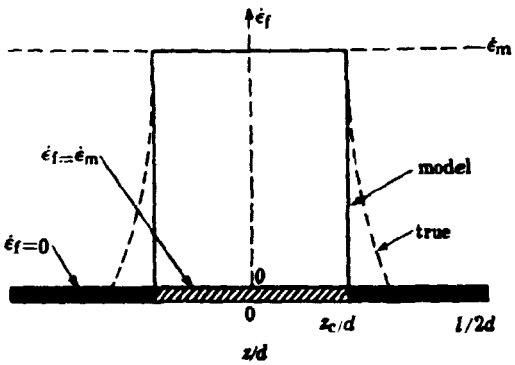

Fig. 8. The fibre creep rate distribution over a fibre length, for the model (Kelly and Street, 1972b).

In the central portion of the fibre, $|z| < z_c$, Kelly and Street take the fibre creep rate and the matrix creep rate to be equal, $\dot{\varepsilon}_f = \dot{\varepsilon}_m$. Near the fibre ends $|z| > z_c$, they assume that the fibre does not creep, $\dot{\varepsilon}_f = 0$. In this way they neglect the creep rate transients in the regions near the points where $|z| = z_c$. If the fibre stress sensitivity is high, such a transient would be very steep, and Kelly and Street therefore expect the approximation to be a good one.

On the basis of this model the shear strain rate of the matrix is, according to eqs. 23 and 24, zero for $|z| < z_c$. The interface shear stress is therefore also zero and following the procedure for the case of non-creeping fibres Kelly and Street obtain the fibre stress distribution

$$\sigma_f = \frac{2n}{n+1}\left(\frac{2}{3a}\right)^{1/n} \sigma_o \left(\frac{\dot{\varepsilon}_c}{\dot{\varepsilon}_o}\right)^{1/n} \left[\left(\frac{1-z_c}{2d}\right)^{\frac{n+1}{n}} - \left(\frac{|z|-z_c}{d}\right)^{\frac{n+1}{n}}\right], \quad |z| > z_c$$

$$\sigma_f = \frac{2n}{n+1}\left(\frac{2}{3a}\right)^{1/n} \sigma_o \left(\frac{\dot{\varepsilon}_c}{\dot{\varepsilon}_o}\right)^{1/n} \left(\frac{1-z_c}{2d}\right)^{\frac{n+1}{n}}, \quad |z| < z_c \tag{33}$$

The distributions for $|z| > z_c$ are the same as in the case of non-creeping fibres (eq. 29) except that they now originate at $|z| = z_c$ rather than at $z = 0$. The parameter, z_c, is determined by the creep strength of the fibres and the creep rate, $\dot{\varepsilon}_c$, of the composite.

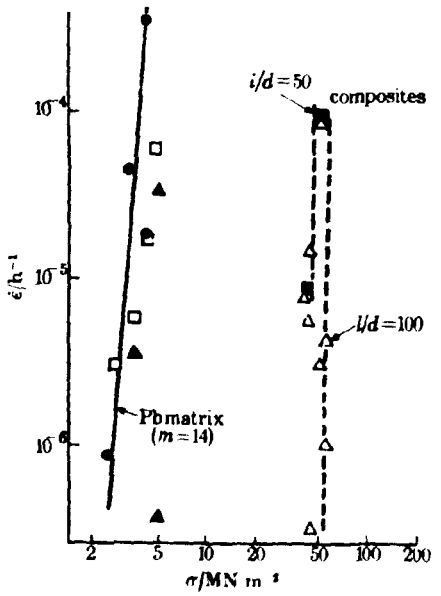

Fig. 9. Stress dependence of the minimum creep rate for unreinforced Pb and discontinuous phosphor bronze wire reinforced Pb, in double logarithmic coordinates. Also shown are data for Pb after Betty (1935) (▲), and after McKeown (1937) (○) (Kelly and Street 1972a).

Experimentally, Kelly and Street (1972a) investigated the creep of lead containing nominally 40 vol% phosphor bronze fibres of aspect ratios 50 or 100 and diameter 450 μm. The composites were fabricated by vacuum infiltration and creep tested in air under constant load at 20°C. Creep data were also obtained for pure lead. The creep curves for the composites

generally displayed well-developed steady-state regions. Fig. 9 shows the measured steady-state (minimum) creep rates versus the applied stress.

Kelly and Street approximate the matrix data by a power law with exponent $n = 14$. The effect of increasing the fibre aspect ratio from 50 to 100 is very small. This is, on the basis of Kelly and Street's model, explained by creep of the fibres.

3.4. McLean

McLean (1972) proposes a model similar to those of Mileiko (1970) and Kelly and Street (1972b). His model refers to the situation where there is neither creep in the fibres nor sliding at the fibre/matrix interface. The main point in his analysis is the assumption that the rate of work done on the composite is equal to the rate of strain energy dissipation in the matrix. He expresses this as

$$\sigma_c \dot{\varepsilon}_c = \bar{\tau} \dot{\bar{\gamma}} V_m , \tag{34}$$

where $\bar{\tau}$ and $\bar{\gamma}$ are the average shear values parallel to the plates. From a geometrical argument he finds that

$$\dot{\bar{\gamma}} = \dot{\varepsilon}_c \frac{1}{2s} .$$

This equation refers to a flow pattern which involves holes at the plate ends. In an attempt to account for this, McLean assumes a doubling of $\bar{\gamma}$ and obtains

$$\dot{\bar{\gamma}} = \dot{\varepsilon}_c \frac{1}{s} . \tag{35}$$

Finally McLean assumes that the matrix creeps according to a power law. To facilitate a comparison with previous treatments I take eq. 8 to be the shear relation

$$\dot{\bar{\gamma}} = \frac{3}{2} \dot{\varepsilon}_o \left(\frac{2\bar{\tau}}{\sigma_o}\right)^n . \tag{36}$$

Combination of eqs. 1, 20, 34, 35 and 36 yields

$$\sigma_c = c V_f \sigma_o \left(\frac{\dot{\varepsilon}_c}{\dot{\varepsilon}_o}\right)^{1/n} \rho^{1+1/n} \tag{37}$$

with

$$c = \frac{1}{2} \left(\frac{2}{3}\right)^{1/n} \left(\frac{V_f}{V_m}\right)^{1/n}$$

McLean emphasizes the fact that the interface shear stress, for higher values of n, is found to be approximately constant. In the presentation of Kelly and Tyson's ideas (section 2.1) this was seen to correspond to a nearly linear σ_f-distribution in the fibre, according to eq. 12. McLean points out that an equation similar to eq. 12 must also apply for the matrix, so that a nearly linear σ_f-distribution can be expected in the matrix, too. He shows that this leads to the situation where fibres/plates and matrix contribute approximately equally to the total load supported by the composite. The high matrix stresses required in this situation are possible without excessive creep-rates in the matrix, because the transverse constraint of the non-creeping fibres generates a transverse tensile stress which partially balances the longitudinal stress (see for example eq. 7).

On this basis, it can be understood that eqs. 13, 21, and 31 are not physically satisfactory, since they underestimate or even ignore the contribution to σ_c from the matrix. By working in terms of energy, McLean avoids discussing the stress system in the matrix. In so doing, he obtains a physically more correct analysis, although it leads to a result which is essentially identical to that of previous analyses.

3.5. Discussion

The preceding slightly simplified presentation of the models by Mileiko (1970), Kelly and Street, (1972b), and McLean (1972), shows that the creep strength predicted by these models on the basis of a power law can in all cases be expressed as

$$\sigma_c = c\, V_f\, \sigma_o \left(\frac{\dot{\varepsilon}_c}{\dot{\varepsilon}_o}\right)^{1/n} \rho^{1+1/n},$$

when the fibres/plates are non-creeping and the interface cohesion is perfect.

This relation can also be obtained by rearrangement of the original expressions. Fig. 10 shows the original creep strength coefficients, c (called α_i in the figure). All the creep strength coefficients are seen to be nearly independent of n when $n \sim 6$. The variation of c with V_f is also seen to be insignificant in the range of V_f between ~ 0.2 and ~ 0.7, which is the range of practical interest. It is therefore reasonable in all cases simply to substitute c by a constant.

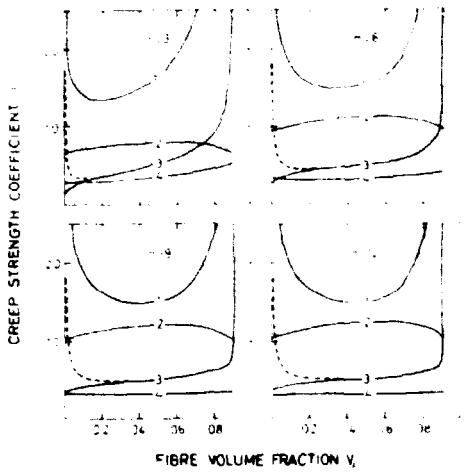

Fig. 10. The creep strength coefficients, σ_i. Index i refers to each curve as indicated (1, McLean, 2, present model, 3, Kelly and Street, 4, Mileiko). Kelly and Street's coefficient has been computed for $\rho = 50$ (dashed curve) and $\rho = \infty$ (solid curve) (Bøcker Pedersen 1974a).

When considering this agreement between the predictions of σ_c, one should bear in mind that there are strong similarities between the creep models. All the models are single element models. In other words, the unit element of composite material selected for analysis consists of a single fibre/plate and an adjacent region of matrix material. This is a reasonable first choice; but whether it provides a true representation of the composite behaviour can perhaps be answered only through experiments.

A more serious simplification in the models appears to be that they are based on a power law for creep of the matrix. The matrix power law leads to a power law for the composite as a whole, and this prediction is not in agreement with for instance the experiments by Kelly and Tyson (1966).

4. THEORY

As it appears from the discussion of the creep law of crystalline solids (section 2), one cannot expect a constant stress sensitivity (i. e. a power law) over a range of $\dot{\epsilon}/D$ greater than that between roughly 10^2 cm^{-2} and 10^9 cm^{-2} (see fig. 1). Furthermore, the experiments by Kelly and Tyson (1966) clearly indicate a composite stress sensitivity that increases with the applied stress. It is therefore important to avoid the assumption of a power law for creep of the matrix when formulating a model for the steady-state creep of composites containing discontinuous aligned fibres. Bilde-

Sørensen, Bøcker Pedersen and Lilholt (1975) in their exploratory study of the influence of the matrix creep law on the creep law of the composite showed that the models by Kelly and Street (1972b) and McLean (1972) could be evaluated on the basis of more general matrix creep laws than the simple power law. However, these models are based upon simple assumptions regarding the average shear strain rate in the matrix. The present model, which does not use these assumptions, is derived from fundamental principles and involves a general matrix creep law.

4.1. Equilibrium Conditions

The basic principle from which the present analysis is derived is that the variations of the components of the stress tensor must satisfy the conditions for static equilibrium. In the axially symmetric case these conditions are expressed by the set of non-trivial equations of equilibrium (see e.g. Timoshenko and Goodier (1951))

$$\sigma_{rz} = \sigma_{zr} \tag{38}$$

$$\frac{\partial \sigma_r}{\partial r} + \frac{\partial \sigma_{rz}}{\partial z} + \frac{\sigma_r - \sigma_\theta}{r} = 0 \tag{39}$$

$$\frac{\partial \sigma_{rz}}{\partial r} + \frac{\partial \sigma_z}{\partial z} + \frac{\sigma_{rz}}{r} = 0 , \tag{40}$$

in which the stress components are defined in fig. 11.

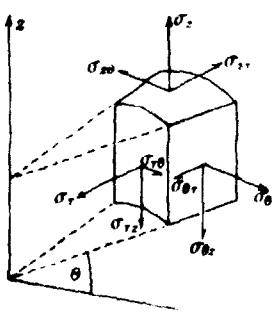

Fig. 11. Components of the stress tensor referred to cylindrical polar coordinates (from Kelly and Groves, 1970).

By integrating eq. 40 with respect to r' between d/2 and r, I obtain

$$2r\,\sigma_{rz}(r) - d\,\sigma_{rz}(d/2) + 2\int_{d/2}^{r} r' \frac{\partial \sigma_z}{\partial z}\, dr' = 0 . \tag{41}$$

Equation 41 is the basis for the simple analysis described in appendix II, where the integral term is neglected. In commenting upon this analysis, Kelly (1973b) notes that it is not exact, since transverse stresses in the matrix are neglected. In a later analysis (Bøcker Pedersen 1974a) the transverse stresses are included via the assumption that the composite load is equally divided between the components (McLean 1972).

These early stress analyses both involve a power law for creep of the matrix, and they essentially confirm the predictions of previous power law models (Bøcker Pedersen 1974a and b).

4.2. Creep Model

The present model involves a general matrix creep law and it refers to the case in which there is no creep in the fibres and no sliding at the fibre/matrix interface. I imagine the composite to consist of a set of parallel identical unit elements randomly distributed in a matrix which creeps under uniaxial stress. The unit element, shown in fig.12, consists of a fibre embedded in a concentric matrix cylinder, in which the transverse stress will be seen to be localized. Like previous models, the present model is therefore a single element model. It also bears some resemblance to the three-component model by Kelly and Lilholt (1969), in the sense that both models involve a division of the matrix into two regions.

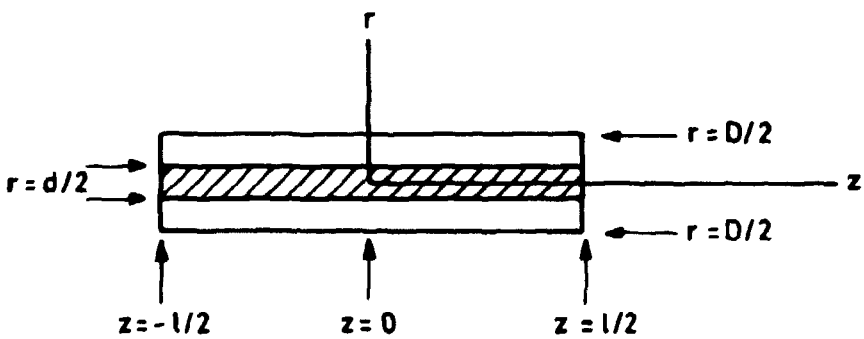

Fig. 12. Unit element and cylindrical polar coordinates.

It can be seen from eq. 41 that the shear stress, $\sigma_{rz}(r, z)$, decreases as r increases, because of the inverse r-dependence and the subtraction of the (positive) integral term. One can therefore expect a more rapid fall-off of σ_{rz} than that corresponding to the inverse r-dependence. Following this I select the following boundary conditions (BC) on the

inner and outer diameters of the unit element

$$\dot{u}_z = 0 \qquad \text{at} \qquad r = d/2 \qquad \text{BC1}$$

$$\dot{u}_z = \dot{\epsilon}_c z \qquad \text{at} \qquad r = D/2 \qquad \text{BC2}$$

$$\sigma_{rz} = 0 \qquad \text{at} \qquad r = D/2 \; . \qquad \text{BC3}$$

I shall assume the matrix cylinder to deform in simple shear, thus approximating the shear strain-rate parallel to the fibre,

$$\dot{\gamma}_{rz} = \frac{\partial \dot{u}_z}{\partial r} + \frac{\partial \dot{u}_r}{\partial z} \; ,$$

by

$$\dot{\gamma}_{rz} = \frac{\partial \dot{u}_z}{\partial r} \; . \qquad (42)$$

This approximation involves holes opening up at the fibre ends. However, except when considering the situation close to a fibre end, this appears to me to be a minor point.

Two important relations may be derived from the prescribed boundary conditions. The first refers to the strain-rate system and is obtained by integration of the approximate $\dot{\gamma}_{rz}$ expression, eq. 42, under the boundary conditions BC1 and BC2. This relation is

$$\dot{\epsilon}_c z = \int_{d/2}^{D/2} \dot{\gamma}_{rz}(r, z)\, dr \; . \qquad (43)$$

The second relation, which refers to the stress system, is obtained by integration of the equilibrium equations under the prescribed boundary condition:

Integration of eq. 40 under BC3 with respect to r between d/2 and D/2 gives

$$d\tau_i = 2 \int_{d/2}^{D/2} r \, \frac{\partial \sigma_z}{\partial z} dr$$

with

$$\tau_i = \sigma_{rz}(d/2) \; .$$

Subsequent integration with respect to z' between 0 and z gives the load, $P_M(z)$, supported by the matrix cylinder

$$P_M(z) - P_M(0) = \int_0^z \int_{d/2}^{D/2} 2\pi r \frac{\partial \sigma_z}{\partial z} \, dr \, dz' = \int_0^z \pi d \tau_i \, dz' \qquad (44)$$

Similarly, the load supported by the fibre is given by

$$P_F(z) - P_F(\tfrac{1}{2}) = \int_z^{1/2} \pi d \tau_i \, dz' \qquad (45)$$

and the load supported by the unit element is

$$P_{UE} = P_F + P_M . \qquad (46)$$

Equation 44 represents the integration indicated by McLean (1972) in his discussion of the distribution of load between fibres/plates and matrix. McLean concludes that for high stress exponents in the matrix power creep law the two components contribute approximately equally to the composite load (equipartition of load). In order to arrive at this conclusion he has to make two assumptions, which in essence are expressed as

$$P_M(0) = 0 \qquad \text{BC4}$$

and

$$P_F(\tfrac{1}{2}) = 0 . \qquad \text{BC5}$$

I shall assume these to be additional boundary conditions. It may be seen from eqs. 44 and 45 that the average values of P_M and P_F along the unit element are identical if τ_i is independent of z. In other words, for high stress sensitivities the present model tends to involve equipartition of load between the fibres and the matrix cylinders. The large tensile stresses associated with this situation require the existence of transverse stresses in the matrix cylinders.

The second important relation involves the composite creep strength, defined as

$$\sigma_c = \bar{\sigma}_{UE} V_{UE} + (1 - V_{UE}) f(\dot{\epsilon}_c) , \qquad (47)$$

where the average tensile stress, $\bar{\sigma}_{UE}$, supported by the unit element is given as

$$\bar{\sigma}_{UE} = \frac{P_{UE}}{\frac{\pi}{4} D^2} \tag{48}$$

and the volume fraction of unit elements as

$$V_{UE} = V_f \left(\frac{D}{d}\right)^2 . \tag{49}$$

Since the matrix embedding the unit elements extends under uniaxial stress, it contributes negligibly to σ_c, so that a good approximation is obtained by

$$\sigma_c = \bar{\sigma}_{UE} V_{UE} . \tag{50}$$

Combination of eqs. 44-46, BC4, BC5 and 48-50 gives

$$\sigma_c = \frac{4 V_f}{d} \int_0^{l/2} \tau_i(z) dz, \tag{51}$$

which is the second important relation.

4.3. Composite Creep Law

By using the intermediate value theorem it is possible to express eqs. 43 and 51 in a form similar to that of the two equations from which Bilde-Sørensen, Bøcker Pedersen and Lilholt (1975) extend the applicability of McLean's model to a general matrix creep law (BBL, eqs. 2 and 5). A similar evaluation is therefore possible for the present model, as will be shown.

The intermediate value theorem states for any function g(x) which is continuous in an interval $a \leq x \leq b$ that at least one value, c, of x exists such that

$$\int_a^b g(x)dx = (b - a)\, g(c)$$

and

$$a \leq c \leq b .$$

The functions $\tau_i(z)$ and $\dot{\gamma}_{rz}(r, z)$ are of course continuous, so the theorem may be applied to eqs. 43 and 51. Equation 51 can therefore be written as

$$\sigma_c = \frac{1}{2} \frac{4V_f}{d} \tau_i(z^{ref}) , \tag{52}$$

where

$$0 \leq z^{ref} \leq \frac{1}{2} .$$

Similarly, by inserting the reference value $z = z^{ref}$ into eq. 43 and applying the intermediate value theorem, one finds

$$\dot{\epsilon}_c z^{ref} = \frac{D-d}{2} \dot{\gamma}_{rz}(r^{ref}, z^{ref}) , \tag{53}$$

where

$$d/2 \leq r^{ref} \leq D/2 .$$

Equations 52 and 53 may be recast as

$$2 \tau^{ref} = 2 \tau_i(z^{ref}) = \frac{\sigma_c}{\rho V_f} \tag{54}$$

and

$$\frac{2}{3} \dot{\gamma}^{ref} = \frac{2}{3} \dot{\gamma}_{rz}(d/2, z^{ref}) = \dot{\epsilon}_c \frac{1}{s} \Phi , \tag{55}$$

where

$$\Phi = \frac{4}{3} \frac{z^{ref}}{l} \frac{\dot{\gamma}_{rz}(d/2, z^{ref})}{\dot{\gamma}_{rz}(r^{ref}, z^{ref})}$$

and

$$s = D-d .$$

The value of z^{ref} depends upon the function $\tau(z)$ which is likely to depend upon the matrix creep law, f, the fibre aspect ratio, ρ , and the composite creep rate, $\dot{\epsilon}_c$. The same applies to r^{ref} and $\dot{\gamma}_{rz}$, so the quantity Φ may depend upon these parameters.

The reference shear values, τ^{ref} and $\dot{\gamma}^{ref}$, are corresponding shear values in the same point $(d/2, z^{ref})$. Consequently, they are related through eq. 11, the general shear relation. Combination of eqs. 11, 54 and 55 gives the composite creep law in the form

$$\frac{\sigma_c}{\rho V_f} = f(\dot{\epsilon}_c \frac{1}{s} \Phi)) . \qquad (56)$$

Equation 56 contains the unknown quantity, Φ. This disadvantage may perhaps be regarded as the cost of the generality of the result. In the following section it will be seen that the previous models, extended to comprise a matrix creep law which is more general than the power law, tend to involve a constant value for Φ.

The equation also contains the parameter, s, which is not determined by the analysis. Such a disadvantage is also inherent in for instance the model by Kelly and Street (1972b), which relies upon an essentially arbitrarily selected value of s. An appropriate value of s is roughly indicated by the velocity profiles obtained by the stress analysis described in appendix II. Judging from the profiles I would expect s to be of the order of d, or probably less, in agreement with the value adopted by Kelly and Street.

4.4. Discussion

In order to make possible a comparison between the expressions predicted by the various models for the composite creep law, it is necessary to evaluate the previous models, which are originally based upon a power law, on the basis of a more general matrix creep law. Bilde-Sørensen, Bøcker Pedersen and Lilholt (1975) evaluate the model by McLean (1972) on the basis of a general matrix creep law. BBL omit the doubling of $\bar{\nu}$ included in the original model, and obtain (BBL, eq. 8)

$$\frac{4 V_f}{1-V_f} \frac{\sigma_c}{V_f 1/s} = f(\dot{\epsilon}_c \frac{1}{s} \frac{1}{3}) . \qquad (57)$$

Lilholt (1975) has pointed out to me that the model by Mileiko (1970) may be extended along the same lines as the model by McLean. For the simple version presented in this report the result is

$$\frac{2 V_f}{1-V_f} \frac{\sigma_c}{V_f 1/s} = \frac{2 \sigma_c}{V_{f\rho}} = f(\dot{\epsilon}_c \frac{1}{s} \frac{1}{3}) \qquad (58)$$

Equations 57 and 58 are, except for a factor of two, identical, and they both involve a constant value of Φ

$$\Phi = 1/3 \quad \text{(Mileiko and McLean)} \qquad (59)$$

It should be remembered, however, that, strictly speaking, the models by Mileiko (in the version presented in this report) and McLean refer to plate composites, although the extension to fibres may appear straight-forward.

The model by Kelly and Street (1972b) refers to a fibre composite. BBL investigate this model for the case in which there is no creep in the fibres and no sliding at the interface. They evaluate the model on the basis of a matrix creep law, f_{PE}, which is either a power law (P) or an exponential law (E) and find the composite creep law (BBL, eq. 21)

$$\frac{2\sigma_c}{\rho V_f} = f_{PE}\left(\dot{\epsilon}_c \frac{1}{s} \frac{2}{3\sqrt{e}}\right) \tag{60}$$

with

$$s = 2\,a\,d,$$

where

$$a = \frac{1}{2}\left[\left(\frac{2\sqrt{3}}{\pi} V_f\right)^{-1/2} - 1\right].$$

The argument of f_{PE} is seen to be of the same form as the argument of f in eq. 56, with

$$\Phi = \frac{2}{3\sqrt{e}} \quad \text{(Kelly and Street)}. \tag{61}$$

BBL discuss the implications of eqs. 57 and 60 on the basis of the $\log \sigma_c$ versus $\log \dot{\epsilon}_c$ curve. Equation 60, for instance, leads to the logarithmic expressions (BBL, eqs. 22 and 23)

$$\log \sigma_c = \log \sigma_M + \log\left(\frac{1}{2}\rho V_f\right) \tag{62}$$

$$\log \dot{\epsilon}_c = \log \dot{\epsilon}_M + \log\left(\frac{s}{l} \frac{3\sqrt{e}}{2}\right). \tag{63}$$

These expressions show that in a $\log\sigma$ versus $\log\dot{\epsilon}$ diagram the composite curve (i. e. $\log \sigma_c$ versus $\log \dot{\epsilon}_c$) is obtained by displacing each point of the matrix curve (i. e. $\log \sigma_M$ versus $\log \dot{\epsilon}_M$) by $\log\left(\frac{1}{2}\rho V_f\right)$ along the $\log\sigma$-axis and by $\log\left(\frac{s}{l} \frac{3\sqrt{e}}{2}\right)$ along the $\log\dot{\epsilon}$-axis. This operation reproduces the shape of the matrix curve in the composite curve, since the displacement vector is the same for all points along the matrix curve.

The more general eq. 56 leads to the logarithmic expressions

$$\log \sigma_c = \log \sigma_M + \log (\rho V_f) \tag{64}$$

$$\log \dot{\epsilon}_c = \log \dot{\epsilon}_M + \log \left(\frac{s}{\Gamma} \frac{1}{\Phi}\right) \tag{65}$$

According to eqs. 64 and 64 the composite curve may also be generated by a displacement of the points of the matrix curve. However, in this case the strain-rate component,

$$\log \left(\frac{s}{\Gamma} \frac{1}{\Phi}\right)$$

of the displacement vector may vary with $\dot{\epsilon}_c$. It is therefore possible that the shape of the composite curve could differ from the shape of the matrix curve; but numerical calculations (Bilde-Sørensen 1975) indicate that for high stress-sensitivities Φ is a slow function of $\dot{\epsilon}_c$, so that the change of shape would be insignificant.

BBL point out that eqs. 57 and 60 suggest a systematic method of handling composite creep date by using generalized diagrams. On the basis of,for instance, eq. 60, such a diagram is obtained by plotting $\log \left(\frac{\dot{\epsilon}_c \rho}{3 \sqrt{e} a}\right)$ versus $\log \left(\frac{2\sigma_c}{\rho V_f}\right)$. This should produce a master curve representing both composite and matrix creep data.

5. EXPERIMENTAL METHODS

The copper-tungsten model system was chosen because its properties include a good interface cohesion, negligible mutual solubility of fibres and matrix, and a large difference between the creep strength of fibres and matrix. The steady-state creep of copper containing discontinuous tungsten fibres can therefore be expected to be described by the theory presented in the foregoing section. Furthermore, extensive data on the creep properties of tungsten (Harris and Ellison 1966 ; Dean 1967 ; Burwood-Smith 1970) and copper (Orlova and Cadek 1970; Pahutova, Cadek and Rys 1971 ; Needham, Wheatley and Greenwood 1975) exist in the literature.

5.1. Specimen Preparation

Cold drawn tungsten wire of diameter 500 μm was obtained from Mullard Ltd., and 99.999% pure copper was supplied by Johnson, Matthey and Co.

Composite rods of diameter 3mm were made by liquid infiltration of the copper around tungsten wires. Before infiltration the tungsten wire was cleaned by boiling in a solution of NaOH for $\frac{1}{2}$ hr, washed in water and acetone and dried, in order to promote a good interface cohesion in the composite. Infiltration was carried out at a temperature of 1150°C under a vacuum better than 10^{-5} torr. The copper matrix was solidified at a rate of approximately 10 cm/hr , yielding a single crystal matrix.

Composites containing continuous fibres of diameter 100 μm were made by infiltration of fibre bundles which were wound on the wire winding machine described by Lilholt (1968).

Composites containing discontinuous fibres of diameter 500 μm were made by infiltration of fibre bundles prepared as follows: the tungsten wire was notched at intervals where it could be easily broken. The distance between the notches was equal to the fibre length. Continuous lengths of the notched wire were then arranged in bundles, held together by copper wire. Bending of the entire bundle would usually break the wires at most of the notches giving a bundle of discontinuous fibres.

Specimens of copper were prepared using the same procedure as for the composite, only omitting the fibres. This method yielded single crystals.

Specimens for creep testing were made by soldering steel balls to the ends of the rods. Soldering was carried out under a vacuum better than 10^{-5} torr at a temperature of 1000°C, using a Nicobraz 10 solder. The distance between the steel balls (i. e. the gauge length, L) was either 45 or 100 mm.

5.2. Testing

Uniaxial constant load creep tests were performed in air at 500°C using a 13:1 ratio lever type creep machine.

The steel balls joined to the ends of the specimen were held in the grips of the creep machine and the extension was measured by connecting the steel balls to a differential transformer via extensometer rods. The relative displacement of the rods was magnified 100 or 200 times and was continuously recorded. The extension, measured in this way, includes a contribution from shear at the steel balls. However, the contribution was found to be negligible in the creep tests of composites containing discontinuous fibres.

The temperature, measured with a thermocouple in contact with the specimen, was held constant within $\pm$ 1°C. The variation along the specimen

was less than $\pm$ 1 °C for L = 45 mm and less than $\pm$ 5°C for L = 100 mm.

There were no indications of oxidation of the fibres even after 1255 hrs. A thin layer of CuO, which tended to crack off (oxide/metal volume ratio = 1.8), was formed on the surface of the composites during the creep test, but this was not expected to influence the creep behaviour significantly.

The composites were examined after the creep tests by dissolution of the matrix in a solution of HNO_3.

6. EXPERIMENTAL RESULTS

The present experiments were made to supplement the few experimental data available to test the predictions of the theory presented in section 4. Creep curves were therefore measured at 500°C for pure copper and for composites of copper containing 28 vol.% tungsten fibres of nominal aspect ratio ρ_{nom} = 25 or ρ_{nom} = 70. Experiments on a few composites with continuous fibres were also conducted in order to look for possible grip shear.

6.1. Pure Copper

The creep curves for pure copper at 500°C did not show steady-state creep, but in the range of 100 - 1000 hrs the variation of the creep-rate was normally found to be within half a decade. The applied stresses and the bounds of $\dot{\varepsilon}$ in the range of 100 - 1000 hours for pure copper are given in table 1 and plotted in fig. 13.

Table 1

Creep of pure copper (T = 500°C, L = 45 mm)

Specimen	σ / MN m^{-2}	$\dot{\varepsilon}$ / h^{-1}
M1	9.8	$1\text{-}3 \times 10^{-4}$
M2	14.7	$1\text{-}4 \times 10^{-4}$
M3	19.6	$1\text{-}2 \times 10^{-3}$
M4	11.8	$2\text{-}4 \times 10^{-5}$

The experimental scatter in the present data for copper may arise from a number of sources. The results obtained by Orlova and Cadek (1979) for creep at 471°C of copper single crystals indicate that differences in the crystallographic orientation of the single crystals can cause a variation of

Table 2

Creep of copper containing 28 vol. % discontinuous tungsten fibres of diameter 500 μm (T = 500°C)

Specimen		σ/MN m^{-2}	$\dot{\varepsilon}$/h^{-1}	t_o/h	t_1/h	t_2/h	p_{nom}	L/mm
C1	1	122.6	1.2×10^{-4}	-	12	24		
C2	2i	78.5	1.9×10^{-5}	-	5	20		
	ii	103.0	2.0×10^{-4}	-	31	42		
	3	103.0	2.0×10^{-5}	-	15	73		
C3	4	122.6	2.8×10^{-5}	-	50	94	25	45
	5i	137.3	1.4×10^{-4}	6	-	-		
	ii	147.2	2.2×10^{-4}	7	-	-		
	iii	157.0	4.4×10^{-4}	11	-	-		
	6	127.5	-	-	-	-		
	7	196.2	-	-	-	-		
C4	8	196.2	5.6×10^{-5}	-	13	49		
	9	186.4	4.1×10^{-4}	5	-	-		
C5	10	206.0	4.2×10^{-4}	6	-	-		
	11i	147.2	$<1.0 \times 10^{-6}$	-	570	683		
	ii	157.0	$1\text{-}2 \times 10^{-6}$	-	380	478	70	45
	iii	176.6	$5\text{-}8 \times 10^{-6}$	-	210	370		
	12i	166.8	$<2.0 \times 10^{-6}$	-	1183	1255		
	ii	196.2	2.0×10^{-5}	-	500	745		
C6	13i	147.2	3.5×10^{-6}	-	100	110		
	ii	166.8	7.5×10^{-5}	-	20	97		
C7	14	157.0	7.5×10^{-6}	-	300	530		
	15	250.2	-	-	-	-		
C8	16i	166.8	6.0×10^{-6}	-	24	50		
	ii	196.2	4.5×10^{-5}	-	55	66	70	100
C9	17i	166.8	4.2×10^{-6}	-	36	110		
	ii	176.6	6.5×10^{-6}	-	190	330		
C10	18	176.6	1.5×10^{-6}	-	70	550		
C11	19i	147.2	7.0×10^{-7}	-	70	330		
	ii	166.8	8.0×10^{-7}	-	350	815		

$\dot{\epsilon}$ which is roughly half a decade. At the small loads required there might also be a contribution from friction in the creep machine. However, as seen in fig. 13, the present results are in fair agreement with those of Pahutova, Cadek and Rys (1972) and Needham Wheatley and Greenwood (1975) for creep at 500°C of pure polycrystalline copper.

6.2. Composites

The creep curves obtained for the composites containing discontinuous fibres generally displayed well-developed regions of steady-state creep. A few curves showed only an inversion point. When steady-state creep had been observed for a time sufficiently long to give a reliable value of $\dot{\epsilon}$, the load was often increased and further measurements of $\dot{\epsilon}$ were made on the same specimen. The results are given in table 2.

Some creep tests were made on composites containing continuous fibres. These test were all terminated when the composites pulled out of one of the steel balls attached to the ends. The measured strain is therefore likely to include a substantial fraction due to grip shear. The apparent creep-rates obtained in these tests are given in table 3.

Fig. 13 shows a double-logarithmic plot of some of the σ and $\dot{\epsilon}$ values given in tables 1, 2 and 3. The diagram clearly demonstrates the increase of creep strength gained by introducing the fibres. It is seen that the composite creep strength increases as ρ_{nom} increases from 25 to 70, and the composites containing continuous fibres are seen to be stronger than those containing discontinuous fibres. These observations are in qualitative agreement with theoretical predictions. The apparent effect of increasing the gauge length from 45 to 100 mm (compare the results for C4-C7 and C8-C11 in fig. 11) will be discussed in the following section.

Table 3

Apparent creep of copper containing continuous tungsten fibres of diameter 100 μm (T = 500°C, L = 45 mm)

Specimen	V_f	σ/MN m^{-2}	$\dot{\epsilon}$/h^{-1}
K1	0.20	245.3	4.9×10^{-5}
K2	0.30	284.5	4.8×10^{-5}
K3	0.35	255.1	4.6×10^{-6}

The points referring to the composites with continuous fibres represent the maximum possible contribution from grip shear. It can be seen that this contribution may be ignored in the case of composites with discontinuous fibres. This is further supported by the fact that the composites with discontinuous fibres all failed within the gauge length.

The creep data for the composites with discontinuous fibres exhibit considerable scatter. This can generally be expected from measurements of composite creep properties (see for instance the discussion by Kelly and Street 1972a). In the present experiments the small number of fibres per

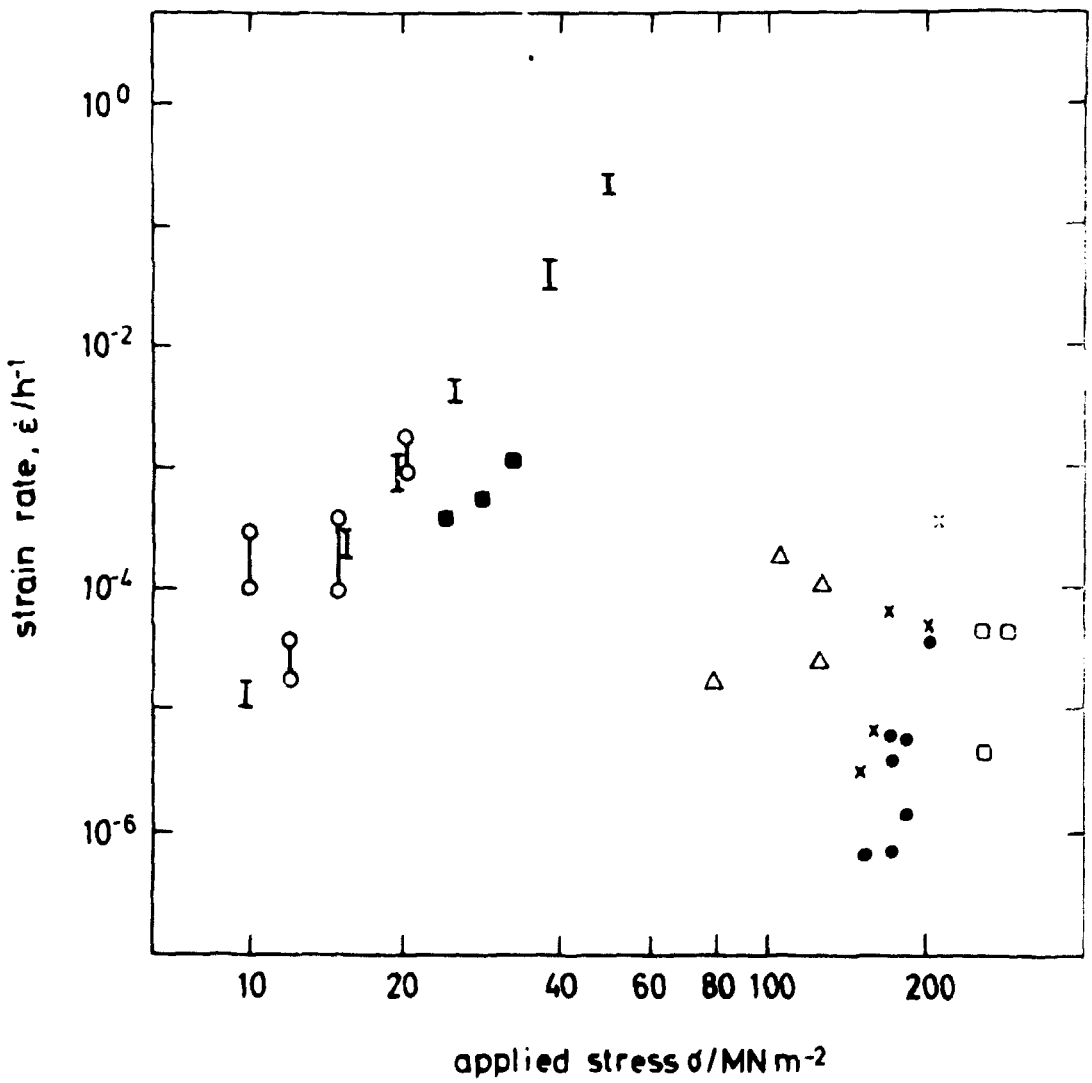

Fig. 13. Experimental data for creep at 500°C of pure copper and copper containing tungsten fibres (see tables 1-4): O, specimens M1-M4; ●, data after Needham, Wheatley and Greenwood (1975); error bars, data after Pahutova, Cadek and Rys (1972); Δ, specimens C1-C3; x, specimens C4-C7; ●, specimens C8-C11; O, specimens K1-K3.

cross section, approximately ten, is responsible for part of the scatter.

A significant additional source of scatter was found by inspection of the fibres in some of the crept composites after matrix dissolution. It was seen that a few of the fibres were still unbroken at some of the notches. Table 4 gives for each specimen the number of fibres containing N = 0, N = 1, N = 2 and N = 3 notches.

Table 4

Characteristics of the fibres in the crept composites

Specimen		N = 0	N = 1	N = 2	N = 3	ρ_{nom}	ρ_{ave}	n_L	L/mm
C1	1	30	10	2	-		33	0	
C2	2	28	6	-	1	25	31	1	45
C3	4	23	6	2	1		35	1	
C4	8	22	-	-	-		70	0	
C5	10	19	1	-	-		74	1	45
C6	13	13	1	1	-		84	2	
C7	14	18	1	-	-	70	74	1	
C8	16	17	3	3	-		97	3	
C9	17	17	6	1	-	70	93	1	100
C10	18	19	6	2	-		96	2	
C11	19	17	4	1	2		105	3	

A linear average, ρ_{ave}, of the aspect ratio was calculated on the basis of the nominal aspect ratio, ρ_{nom}, and N. This value is given in table 4 together with the observed number, n_L, of fibres of length equal to the specimen length. A possible correlation between n_L and σ_c was looked for, but none was found. The difference between ρ_{nom} and ρ_{ave} is in many cases quite large. Consequently, in interpreting the creep data, I have considered only the results for specimens C1-C11, for which a value of ρ_{ave} was obtained.

In all cases composite rupture involved a few fibre ruptures. These were of the cup and cone type and were therefore clearly distinguishable from the original fibre ends. Fibre rupture occurred only at the rupture surface, so the fibres, including those containing notches, seemed to stay intact during steady-state creep.

7. DISCUSSION

The diagram shown in fig. 11 indicates a comparatively low stress sensitivity for the pure copper, a higher stress sensitivity for the composites with $\rho_{nom} = 25$, and a very high stress sensitivity for the composites with $\rho_{nom} = 70$. This is in qualitative agreement with the prediction of the analysis by Bilde-Sørensen, Bøcker Pedersen and Lilholt (1975).

When interpreting the results in greater detail, the presence in the composites of fibres of aspect ratio greater than the nominal value, ρ_{nom}, must be considered. Table 4 shows that most of the fibres in the composites do not contain unbroken notches; in other words, their aspect ratio is equal to ρ_{nom}. For the moment I shall therefore assume that all the fibres have the nominal aspect ratio and estimate the maximum tensile stress as follows:

I determine the average fibre stress by supposing the total composite load to be equally divided between fibres and matrix. Following the analysis by McLean (1972) and the present analysis, this gives

$$\sigma_c = 2 V_f \bar{\sigma}_f , \tag{66}$$

where $\bar{\sigma}_f$ is defined by eq. 14. Taking the interface shear stress to be approximately constant, I have

$$\sigma_f^{max} = 2 \bar{\sigma}_f \tag{67}$$

and hence, by combining eqs. 66 and 67

$$\sigma_f^{max} = \frac{\sigma_c}{V_f} . \tag{68}$$

Using the σ_c-values listed in table 2, I find that σ_f^{max} lies roughly between 280 and 736 MN m^{-2} for a fibre of aspect ratio ρ_{nom}. Extrapolation of the creep rupture data of Harris and Ellison (1966) and of McDanels and Signorelli (1966) shows that creep of tungsten at 500°C can be expected to occur at stresses exceeding roughly 1100 MN m^{-2}. The creep of the fibres of the nominal aspect ratio should therefore be negligible.

However, for an approximately constant interface shear stress, σ_f^{max} is nearly proportional to ρ. The few fibres of aspect ratio $2\rho_{nom}$, $3\rho_{nom}$

or $4\rho_{nom}$ therefore experience maximum stresses which are roughly 2, 3 or 4 times greater than those given by eq. 68. Comparing again with the creep strength, 1100 MN m^{-2}, of tungsten, it appears that creep can be expected around the fibre midpoint when $\rho = 2\rho_{nom}$, while a substantial portion of the fibre should creep when $\rho = 3\rho_{nom}$. This conclusion is supported by the observation of ductile fibre rupture. Furthermore, creep in the long fibres provides an explanation of the fact that no correlation was found between n_L and σ_c.

The influence of the fibres with $\rho = 3\rho_{nom}$ therefore appears to be limited for two reasons: firstly, their small number (less than ~10% of the total number of fibres in a specimen) and, secondly the occurrence of creep in their central part. In view of this I expect creep of the composites to be governed essentially by the fibres of aspect ratio ρ_{nom} and $2\rho_{nom}$ in which the creep is insignificant.

The creep theories refer to composites with fibres of identical length and they cannot therefore be directly applied to the present results. However, in most of the theories the creep strength is given by an equation of the form of eq. 66, where $\bar{\sigma}_f$ is approximately proportional to ρ (when the stress sensitivity is not too small). In order to approximately account for the creep of composites in which ρ has a distribution of values, one might therefore simply replace ρ by the linear average, ρ_{ave}. Strictly speaking, this approach is only valid if none of the fibres experience creep, but I shall use it in dealing with the present data since creep is only significant in a few of the fibres.

Values of ρ_{ave} were obtained for the specimens numbered C1-C11, as seen in table 4, so a quantitative comparison to theoretical predictions is possible for these specimens. This comparison may be made using the diagram suggested by Bilde-Sørensen, Bøcker Pedersen and Lilholt (1975). Fig. 14 shows such a diagram based upon eq. 59. The points for the matrix and those for the composites are seen, within the scatter, to produce a master curve reasonably well. The scatter of data points referring to specimens of the same nominal constitution (specimens C1-C3, C4-C7 and C8-C11) tends to be less than that seen in fig. 13. This shows that part of the scatter can indeed be attributed to differences in the value of ρ_{ave}.

In fig. 13 the data points referring to specimens C8-C11 lie to the right of those referring to specimens C4-C7. No such trend is exhibited in fig. 14. The trend in fig. 13 therefore seems to be due to the fact that ρ_{ave} is generally greater for specimens C8-C11, and not to an effect of the gauge length.

On the other hand, in fig. 14 the data points referring to specimens C1-C3 lie to the right of those referring to specimens C4-C11. This would appear to suggest that the theory overestimates the influence of aspect ratio. However, a recent, detailed calculation by Lilholt (1975), based upon creep data for tungsten by Harris and Ellison (1966), Dean (1967) and Burwood-Smi (1970), indicates that this trend may be attributed solely to creep in the fibre

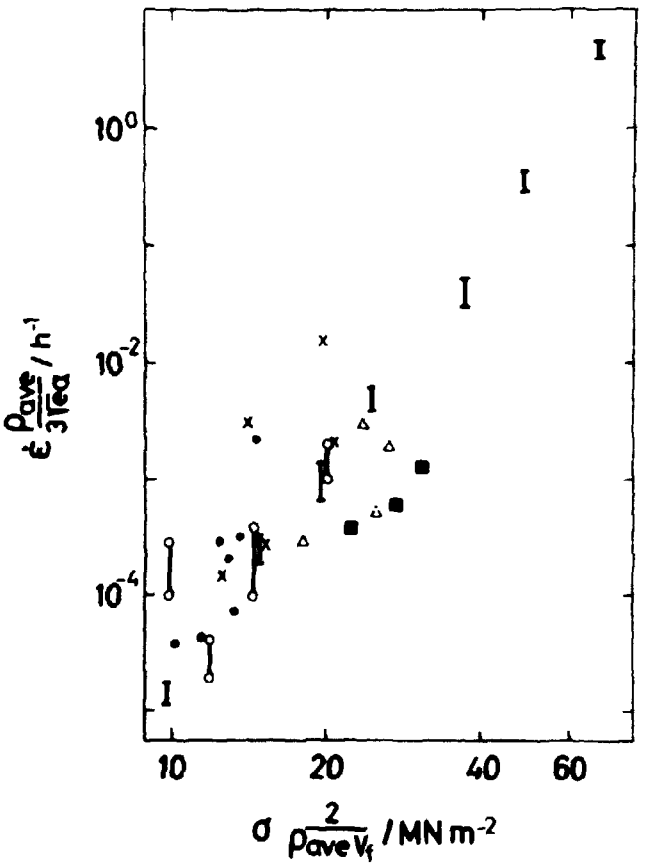

Fig. 14. The data for creep at 500°C of pure copper containing discontinuous tungsten fibres shown in a generalized diagram. The data points refer to the same specimens as in fig. 13.

8. SUMMARY AND CONCLUSIONS

Existing models for the steady-state creep of composites containing aligned discontinuous fibres have been compared. The creep strength predicted by each model on the basis of a power law for creep of the matrix can be expressed by

$$\sigma_c = c\, V_f\, \sigma_o \left(\frac{\dot{\varepsilon}_c}{\dot{\varepsilon}_o}\right)^{1/n} \rho^{1+1/n}$$

in the case where the fibres do not creep. It has been shown that the creep strength coefficient, c, is in all cases approximately constant in the range of parameters of practical interest.

A model has been suggested for predicting the composite creep law from the matrix creep law given in a general form. The predicted composite creep law in the case where the fibres do not creep,

$$\frac{\sigma_c}{\rho V_f} = f\left(\dot{\varepsilon}_c \frac{1}{s} \Phi\right),$$

is essentially identical to the creep law predicted by previous models when these are extended to comprise a general matrix creep law. The previous models involve a constant value for Φ, so that the shape of the predicted $\log \sigma_c$ versus $\log \dot{\varepsilon}_c$ curve should be identical to that of the $\log \sigma_M$ versus $\log \dot{\varepsilon}_M$ curve.

Pure copper and composites consisting of aligned discontinuous or continuous fibres in a copper matrix have been creep tested at 500°C. The creep curves for the composites containing discontinuous fibres generally display well-developed regions of steady-state creep. The creep strength and the stress sensitivity are found to increase with the aspect ratio of the fibres, in qualitative agreement with the theoretical prediction.

A quantitative comparison between theory and experiment has been made by plotting $\log\left(\frac{2\sigma_c}{\rho V_f}\right)$ versus $\log\left(\dot{\varepsilon}_c \frac{\rho}{3\sqrt{e}\, a}\right)$ for the composites together with $\log \sigma_M$ versus $\log \dot{\varepsilon}_M$ for the pure copper. Plotted in this way, the creep data are seen, within the scatter, to produce a master curve reasonably well, in agreement with the theoretical prediction. A slight overestimate of the effect of ρ is expected to result from creep of the fibres.

REFERENCES

Ardell, A.J., and Sherby, O.D., The Steady-State Creep of Polycrystalline Alpha Zirconium at Elevated Temperatures. Trans. AIME 239 (1967) 1547-1556.

Ashby, M.F., The Deformation of Plastically Non-homogeneous Alloys. In: Strengthening Methods in Crystals. Edited by Kelly, A. and Nicholson, R.B. (Elsevier, London, 1971) 137-192.

Ashby, M.F., A First Report on Deformation Mechanism Maps. Acta Met. 20 (1972) 887-897.

Bilde-Sørensen, J.B., Bøcker Pedersen, O., and Lilholt, H., Prediction of the Creep Properties of Discontinuous Fibre Composites from the Matrix Creep Law. Risø-M-1810 (1975) 24 pp.

Bilde-Sørensen, J.B., Risø, Denmark, unpublished work, 1975.

Bird, J.E., Mukherjee, A.K., and Dorn, J.E., Correlations between High-Temperature Creep Behavior and Structure. In: Quantitative Relation between Properties and Microstructure. Proceedings of an International Conference, Haifa, July 27-August 4, 1969. Edited by Brandon, D.G., and Rosen, A. (Israel Universities Press, Jerusalem, 1969) 255-342.

Bøcker Pedersen, O., Creep Strength of Discontinuous Fibre Composites. J. Mat. Sci. 9 (1974a) 948-952.

Bøcker Pedersen, O., On a Constraint Effect in Steady-State Creep of Fibre Composites. In: Composites - Standards, Testing and Design. National Physical Laboratory, 8-9 April 1974b. Conference Proceedings (IPC Science and Technology Press, Guildford, 1974) 33-35.

Bøcker Pedersen, O., Steady-State Creep of Copper-Tungsten Fibre Composites. To appear in: Proceedings of the International Conference on Composite Materials, Geneva, 7-11 April 1975, and Boston Mass., 14-18 April 1975.

Burwood-Smith, A., Mechanical Properties of Refractory Metal Wires for High Temperature Reinforcement. Fibre Sci. Technol. 3 (1970) 105-117.

Cheskis, H. P., and Heckel, R. W., In Situ Measurements of Deformation Behaviour of Individual Phases in Composites by X-ray Diffraction. ASTM-STP-438 (1968) 76-91.

Crouch, A. G., High-Temperature Deformation of Polycrystalline Fe_2O_3. J. Amer. Ceram. Soc. 55 (1972) 558-563.

Dean, A. V., The Reinforcement of Nickel-Base Alloys with High-Strength Tungsten Wires. J. Inst. Metals, 95 (1967) 79-86.

de Silva, A. R. T., A Theoretical Analysis of Creep in Fibre Reinforced Composites. J. Mech. Phys. Solids, 16 (1968) 169-186.

Garmong, G., and Shepard, L. A., Matrix Strengthening Mechanisms of an Iron Fiber-Copper Matrix Composite as a Function of Fibre Size and Spacing. Met. Trans. 2 (1971) 175-180.

Harris, B., and Ellison, E. G., Creep and Tensile Properties of Heavily Drawn Tungsten Wire. ASM Trans. Quart. 59 (1966) 744-754.

Hay, K. A., and Pascoe, R. T., Interdependent Processes in High Temperature Deformation. J. Mat. Sci. 9 (1974) 1285-1289.

Jeffreys, H., Cartesian Tensors (The University Press, Cambridge, 1963) 92 pp.

Kelly, A., Particle and Fibre Reinforcement. In: Strengthening Methods in Crystals. Edited by Kelly, A., and Nicholson, R. B. (Elsevier, London, 1971a)433-484.

Kelly, A., Microstructural Parameters of an Aligned Fibrous Composite. In: The Properties of Fibre Composites. National Physical Laboratory, 4 November 1971b. Conference Proceedings (IPC Science and Technology Press, Guildford, 1974) 5-14.

Kelly, A., Reinforcement of Structural Materials by Long Strong Fibres. Met. Trans. 3 (1972a) 2313-2325.

Kelly, A., Strong Solids 2nd ed. (Clarendon Press, Oxford, 1973a) 285 pp.

Kelly, A., Creep of Composites. In: The Microstructure and Design of Alloys. Proceedings of the Third International Conference on the Strength of Metals and Alloys, Cambridge, 20-25 August 1973b (Institute of Metals, London, 1973) 106-107.

Kelly, A., and Groves, G. W., Crystallography and Crystal Defects (Longman, London, 1970) 428 pp.

Kelly, A., and Lilholt, H., Stress-Strain Curve of a Fibre-reinforced Composite. Phil. Mag. 20 (1969) 311-328.

Kelly, A., and Street, K. N., Creep of Discontinuous Fibre Composites I. Experimental Behaviour of Lead-Phosphor Bronze. Proc. Roy. Soc. A328 (1972a) 267-282.

Kelly, A., and Street, K. N., Creep of Discontinuous Fibre Composites II. Theory for the Steady-State. Proc. Roy. Soc. A328 (1972b) 283-293.

Kelly, A., and Tyson, W. R., Tensile Properties of Fibre Reinforced Metals II. Creep of Silver-Tungsten. J. Mech. Phys. Solids 14 (1966) 177-186.

Lilholt, H., Work Hardening and Fibre Reinforcement. Dissertation, University of Cambridge, 1968.

Lilholt, H., Review of Creep Theories for Fibre Composites. In: High Temperature Materials Phenomena. Proceedings of the Third Nordic High-temperature Symposium, Risø, 7-9 June 1972. Edited by Rasmussen, J. G., (Polyteknisk Forlag, København, 1973) 189-209.

Lilholt, H., Matrix Properties in a Fibre Composite with Metallic Matrix. In: The Microstructure and Design of Alloys II. Proceedings of the Third International Conference on the Strength of Metals and Alloys, Cambridge, 20-25 August 1973. (Institute of Metals, London, 1973) 237-242.

Lilholt, H., Risø, Denmark, Personal communication, 1975.

McCormick, P. G., and Ruoff, A. L., Creep under High Pressures. In: The Mechanical Behaviour of Materials under Pressure. Edited by Pugh, H. L. D. (Elsevier, London, 1970) 355-366.

McDanels, D. L., and Signorelli, R. A., Stress Rupture Properties of Tungsten Wire from 1200° to 2500°F. NASA-TN-D-3467 (1966) 22 pp.

McDanels, D. L., Signorelli, R. L., and Weeton, J. W., Analysis of Stress-Rupture and Creep Properties of Tungsten Fibre Reinforced Copper Composites. ASTM-STP-427 (1967) 124-148.

McLean, D., Viscous Flow of Aligned Composites. J. Mat. Sci. 7 (1972) 98-104.

Mileiko, S. T., Steady-State Creep of a Composite Material with Short Fibres. J. Mat. Sci. 5 (1970) 254-261.

Needham, N. G., and Greenwood, G. W., The Creep of Copper under superimposed Hydrostatic Pressure. Met. Sci. 9 (1975) 258-262.

Needham, N. G., Wheatley, J. E., and Greenwood, G. W., The Creep Fracture of Copper and Magnesium. Acta Met. 23 (1975) 23-27.

Odquist, F. K. G., Mathematical Theory of Creep and Creep Rupture (Clarendon Press, Oxford, 1966) 168 pp.

Orlova, A., and Cadek, J., On the Orientation Dependence of High-Temperature Creep Behaviour of Copper Single Crystals. Phil. Mag. 21 (1970) 923-929.

Pahutova, M., Cadek, J., and Rys, P., High Temperature Creep in Copper. Phil. Mag. 23 (1971) 509-517.

Pascoe, R. T., A Stress Relaxation Technique for Oxides. Trans. Brit. Ceram. Soc. 73 (1974) 143-146.

Sherby, O. D., and Burke, P. M., Mechanical Behaviour of Crystalline Solids at Elevated Temperature. Prog. in Mat. Sci. 13 (1967) 390 pp.

Street, K. N., Steady-State Creep of Fibre-Reinforced Materials. In: The Properties of Fibre Composites. National Physical Laboratory, 4 November 1971b. Conference Proceedings (IPC Science and Technology Press, Guildford, 1974) 36-46.

Stuhrke, W. F., The Mechanical Behaviour of Aluminum-Boron Composite Material. ASTM-STP-438 (1968) 108-133.

Timoshenko, S., and Goodier, J. N., Theory of Elasticity, 2nd ed. (McGraw-Hill, New York, 1951) 506 pp.

APPENDIX I

LIST OF SYMBOLS

A_{ij}	Tranformation matrix
a	Geometrical parameter
B	Creep strength coefficient
D	Diffusion coefficient or geometrical parameter (diameter of unit element)
D_o	Pre-exponential factor
d	Diameter of fibre
δt	Time interval corresponding to the displacements δu_m, δu_i, δu_f and δu_s
δu_m δu_i δu_f δu_s	Displacement of points in the matrix (m), at the interface (i), in the fibre (f), and resulting from sliding (s)
δ_{ij}	Kronecker symbol
E	Activation energy for diffusion
e	Base of the natural logarithm
$\dot{\varepsilon}$	Tensile strain-rate (in the present text, usually the steady-state creep-rate)
$\dot{\varepsilon}_{ij}$	Strain-rate tensor, referred to cartesian coordinates
$\dot{\varepsilon}_c$	Strain-rate of composite
$\dot{\varepsilon}_o$	Constant in power law
$\dot{\varepsilon}_f$	Strain-rate of fibre
$\dot{\varepsilon}_M$	Strain-rate of unreinforced matrix
f	Any continuous function
f_E	Exponential function
f_P	Power function
f_{PE}	Power or exponential function
Φ	Quantity in expression for composite creep law
G	Elastic shear modulus
g(x)	Continuous function of x
$\dot{\gamma}$	Shear strain-rate

$\bar{\dot{\gamma}}$	Average shear strain-rate
$\dot{\gamma}_{r\theta}\dot{\gamma}_{rz}\dot{\gamma}_{\theta z}$	Shear strain-rates referred to polar cylindrical coordinates
h	Thickness of zone of constant shear strain-rate
k	Boltzmann constant
L	Gauge length of specimen. In Mileiko's (1970) notation L is the length of fibres/plates
l	Length of fibre/plate
l'	Overlap of fibres/plates
Λ	Spacing between fibres
N	Number of notches in a fibre
n	Stress exponent in power law
n_L	Number of fibres of length equal to the specimen length
v	Rate of relative displacement of plates/fibres
$0\text{-}x_i$	Cartesian coordinate axes
Ω	Volume for diffusion
P	Hydrostatic stress
$P_F(z)$	Tensile load supported by fibre
$P_M(z)$	Tensile load supported by matrix cylinder
P_{UE}	Tensile load supported by unit element
r	Polar cylindrical coordinate (radial distance from fibre axis)
r^{ref}	Reference value of r
ρ	Aspect ratio of fibres/plates
ρ_{ave}	Average aspect ratio of fibres
ρ_{nom}	Nominal aspect ratio of fibres
s	Geometrical parameter. For plate composites s is the spacing between plates, and for fibre composites s = D-d
s_{ij}	Stress deviator
σ	Tensile stress
σ_o	Constant in power law
$\sigma_1\sigma_2\sigma_3$	Principal stresses

σ_c	Tensile stress in composite
σ_e	Effective stress
σ_f	Tensile stress in fibre
$\bar{\sigma}_f$	Average tensile stress in fibre
σ_f^{max}	Maximum tensile stress in fibre
σ_{ij}	Stress tensor referred to cartesian coordinates
σ_L	Longitudinal tensile stress
σ_M	Tensile stress applied to unreinforced matrix
$\bar{\sigma}_m$	Average tensile stress in matrix
$\sigma_r \sigma_\theta \sigma_z$	Components of the stress tensor referred to polar cylindrical
$\sigma_{r\theta} \sigma_{rz} \sigma_{\theta z}$	coordinates
σ_T	Transverse tensile stress
$\bar{\sigma}_{UE}$	Average tensile stress supported by unit element
T	Absolute temperature
T_m	Absolute melting temperature
t	Thickness of plate
τ	Shear stress
$\bar{\tau}$	Average shear stress
τ_i	Shear stress at the fibre/matrix interface
θ	Polar cylindrical coordinate (angle)
$\dot{u}_m \dot{u}_i$	Rate of displacement of points in matrix (m) and at the interface (i)
$\dot{u}_r \dot{u}_\theta \dot{u}_z$	Displacement rates referred to polar cylindrical coordinates
V_f	Volume fraction of fibres
V_m	Volume fraction of matrix
V_{UE}	Volume fraction of unit elements
z	Polar cylindrical coordinate (distance along the fibre from the fibre midpoint)
z_c	Half the length of central creeping portion of fibre
z^{ref}	Reference value of z

APPENDIX II

INTERFACE SHEAR STRESS[x)]

I consider a discontinuous non-creeping fibre embedded in an infinite matrix. Far from the fibre the matrix is in a condition of uniform steady-state creep at the rate of $\dot{\epsilon}$ in the direction of the fibre axis and I assume that no sliding occurs at the interface between fibre and matrix.

1. Equilibrium Condition

The circular slice of matrix material shown in fig. 1 experiences forces resulting from shear and tensile stresses, as defined in the figure.

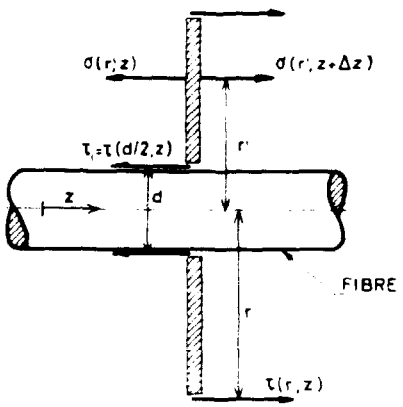

Fig. 1. The stresses acting on a thin circular slice of matric material.

Under static equilibrium the sum of these forces vanishes, giving

$$2r\tau - \tau_i d + 2\int_{d/2}^{r} r' \frac{\partial \sigma}{\partial z}\, dr' = 0 .$$

If the aspect ratio of the fibre is not too small I feel justified in ignoring stress concentrations at fibre ends as well as ignoring the integral term resulting from the variation of tensile stress along the fibre direction.

---

x) Excerpts from personal communication (1973) to Dr. A. Kelly, National Physical Laboratory, London, and Dr. K.N. Street, Ecole des Mines, Paris.

The shear stress then becomes

$$\tau(r,z) = \frac{\tau_i d}{2r} \quad . \tag{1}$$

2. Velocity Profile

The shear strain rate is defined

$$\dot{\gamma} = \frac{\partial \dot{u}}{\partial r} \quad , \tag{2}$$

where $\dot{u}(r,z)$ is the creep velocity relative to the fibre. I assume the stress to be related to the strain rate via a power law

$$\dot{\gamma} = \dot{\gamma}_o \left(\frac{\tau}{\tau_o}\right)^m \quad , \tag{3}$$

where $\dot{\gamma}_o$, τ_o and m are independent of stress. Combination of eqs. 1, 2 and 3 gives

$$\frac{\partial \dot{u}}{\partial r} = \dot{\gamma}_i \left(\frac{d}{2r}\right)^m \tag{4}$$

where

$$\dot{\gamma}_i = \dot{\gamma}_o \left(\frac{\tau_i}{\tau_o}\right)^m \quad .$$

Integration of eq. 4 under the boundary condition that there is no relative velocity between fibre and matrix at the interface gives

$$\dot{u} = \dot{u}^* \left[1 - \left(\frac{2r}{d}\right)^{1-m}\right] \tag{5}$$

where

$$\dot{u}^* = \frac{d}{2} \frac{\dot{\gamma}_i}{m-1} \quad .$$

The reduced velocity, $\dot{u}/\dot{u}^*$, is plotted as a function of r/d for fixed values of m in fig. 2 demonstrating how rapidly the velocities converge to the asymptotic value.

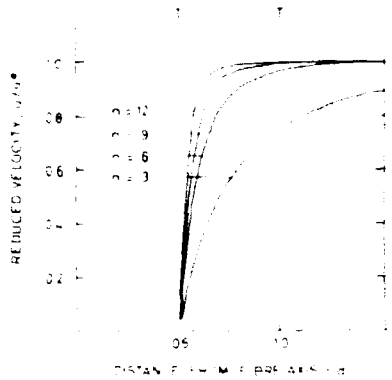

Fig. 2. Profiles of reduced velocities, u/u^{M}, adjacent to the fibre-matrix interface.

3. Interface Shear Stress

The interface stress may be obtained from eq. 5 because, in the normal cases when $m > 1$, one has

$$\dot{u}(r, z) \rightarrow \dot{\epsilon} z \qquad \text{as} \quad r \rightarrow \infty \tag{6}$$

with $z = 0$ at the fibre midpoint. Hence from eqs. 5 and 6

$$\tau_i = (m-1)^{1/m} \tau_o \left(\frac{2\dot{\epsilon}}{\dot{\gamma}_i}\right)^{1/m} \left(\frac{z}{d}\right)^{1/m} \tag{7}$$

The power relation is usually expressed in terms of tensile stress and strain rate

$$\dot{\epsilon} = \dot{\epsilon}_o \left(\frac{\sigma}{\sigma_o}\right)^n$$

and by taking the relations employed by Kelly and Street,

$$\dot{\gamma}_o = \frac{3}{2} \dot{\epsilon}_o , \qquad \tau_o = \frac{1}{2} \sigma_o , \qquad m = n ,$$

the interface stress can be written in the form

$$\tau_i = \beta \sigma_o \left(\frac{\dot{\epsilon}}{\dot{\epsilon}_o}\right)^{1/n} \left(\frac{z}{d}\right)^{1/n} \tag{8}$$

where

$$\beta = \frac{1}{2} \left(\frac{4}{3}\right)^{1/n} (n-1)^{1/n} .$$

4. Discussion

This expression is identical to that obtained by Kelly and Street when the coefficient β is taken as

$$\beta^{KS} = \frac{1}{2}\left(\frac{4}{3}\right)^{1/n} \left[\left(\frac{2\sqrt{3}}{\pi} V_f\right)^{-1/2} - 1\right]^{-1/n} .$$

A comparison between the two theories can be made from fig. 3, where the ratio,

$$\frac{\tau_i}{\tau_i^{KS}} = \frac{\beta}{\beta^{KS}} ,$$

is plotted as a function of V_f for some values of n.

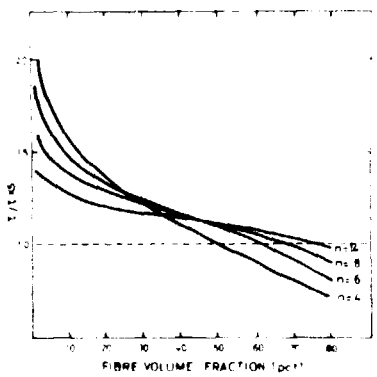

Fig. 3. Ratio between the interface stress predicted by the present theory and by Kelly and Street's. The greatest difference occurs at small values of the volume percent of fibres.

The agreement is good for large values of n when V_f is greater than about 20%. This is not surprising since, as Kelly and Street point out, the value taken for n is not critical for large values of n provided V_f is not too small. But the difference between the theories appears for all values of n when V_f is less than about 20%. In this region I expect the present model to better represent the composite, since the assumption of an infinite matrix should not be critical here.

Reference

A. Kelly and K.N. Street, Creep of Discontinuous Fibre Composite II. Theory for the Steady-State, Proc. Roy. Soc. A328 (1972) 283-293.

APPENDIX III

JOURNAL OF MATERIALS SCIENCE 9 (1974) 948–952

Creep strength of discontinuous fibre composites

O. BØCKER PEDERSEN

Metallurgy Department, Danish Atomic Energy Commission, Research Establishment Risø, DK-4000 Roskilde, Denmark and Department of Structural Properties of Materials, The Technical University of Denmark, DK-2800 Lyngby, Denmark

A unidirectional, discontinuous fibre composite is considered under conditions of steady state creep in the direction of reinforcement. The composite consists of noncreeping, discontinuous, perfectly aligned, uniformly distributed fibres which are perfectly bonded to a matrix obeying a power relation between stress and strain rate. Expressions for the interface stress, the creep velocity profile adjacent to the fibres and the creep strength of the composite are derived. Previous results for the creep strength, σ_c, obtained for composites of the same type are briefly reviewed and compared with the present result. It is shown that all results reduce to the same general expression

$$\sigma_c = \kappa V_f \sigma_m \left(\frac{\dot{\epsilon}}{\dot{\epsilon}_m}\right)^{1/n} \rho^{1-1/n}$$

in which ρ is the fibre aspect ratio, $\dot{\epsilon}$ is the composite creep rate, V_f is the fibre volume fraction, σ_m, $\dot{\epsilon}_m$ and n are the constants in the matrix creep law. The creep strength coefficient κ is found to be very weakly dependent on V_f and practically independent of n when n is greater than about 6.

1. Introduction

It has become well established over the past decade that the resistance to creep at elevated temperatures of a metal matrix can be enhanced by the addition of creep resistant fibres [1–4]. Considerable effort has, therefore, been directed toward the development of mathematical models describing this enhancement in terms of the parameters specifying the constitution of the composite.

Mileiko [5] proposes a model which extends under simple shear of the matrix and with no matrix contribution to the tensile load supported by the model. A small matrix contribution is included in Kelly and Street's model [6] which is based on the assumption of a uniform shear strain-rate in the matrix. McLean [7] employs the same assumption, but derives the creep strength from an energy consideration, and points out that the matrix contribution usually is fairly large. In fact, he concludes that the tensile load is approximately equally divided between fibres and matrix independently of relative volume fractions, as long as flow occurs in the matrix. This is a result of the constraint effect observed in tensile experiments by Kelly and Lilholt [8]. As the matrix deforms plastically, its transverse contraction is constrained by the surrounding fibres which are normally less compliant. In Kelly and Lilholt's experiments this caused a very high apparent tensile stress in the matrix, which disappeared when the fibres yielded, and hence the transverse contractions became the same.

2. The model composite

The approach described here is based on a model which we define by a number of assumptions. The model consists of a matrix containing noncreeping, aligned, cylindrical fibres of diameter d and of length l. The aspect ratio $\rho = l/d$ is assumed to be sufficiently large that end effects may be ignored. The distribution of the fibres is random in a direction parallel to the fibre axis. In cross-sections normal to the fibre axes the fibres are uniformly distributed so as to form a hexagonal array.

The creep behaviour of the matrix is assumed

to be described by the usual power relation

$$\dot{\gamma} = \gamma_0 \left(\frac{\tau}{\tau_0} \right)^n \qquad (1)$$

relating the shear strain-rate, $\dot{\gamma}$, to the shear stress τ. The constants, γ_0, τ_0, and n are related to those obtained in a tensile creep test, ϵ_0, σ_0, and m, by [6]

$$\gamma_0 = \frac{3}{2} \epsilon_0, \tau_0 = \frac{1}{2} \sigma_0, n = m \qquad (2)$$

The adhesion between fibres and matrix is thought to be perfect, so that no relative sliding can occur at the interfaces during creep of the composite.

2.1. The stress system

In a condition of steady state creep the matrix is assumed to extend at the constant rate, $\dot{\epsilon}$, at points midway between two fibres. Taking $z = 0$ at a fibre centre (Fig. 1) this results in a velocity $\dot{\epsilon} z$ relative to the rigid fibre. Since unlimited interface strength is assumed, the relative velocity must decrease to zero at the interface. This is what causes load to be exchanged between the components by means of the interface stress, τ_i. Previous authors [5-7] all found that the interface stress is nearly constant along the major portion of the fibre length when the stress exponent, n, is greater than about 4. Since the tensile load on the fibre is found by integrating τ_i from the fibre end to the point in question, this results in a nearly linear variation of the tensile load on the fibre along its length.

In discussing the distribution of tensile load between the components, McLean points out that the tensile load on the matrix can be obtained by a similar integration of τ_i from the fibre centre. For higher n-values the tensile load in the matrix consequently rises almost linearly from the fibre centre. McLean further concludes that the tensile load of the composite is roughly equally divided between matrix and fibres irrespective of volume fractions. This is in marked contrast to the case in which the matrix does not yield plastically. Here there is normally a preferential loading of the fibres.

In view of the above it appears that reasonable simple assumptions regarding the stress system can be stated by the following:

1. the tensile stress supported by the matrix varies linearly from fibre centre to fibre end at a constant rate given by

$$\frac{\partial \sigma}{\partial z} = \frac{2\sigma_m}{l} \qquad (3)$$

where σ_m denotes the greatest tensile stress in the matrix;

2. the tensile load carried by the composite is nearly equally divided between the components at any fibre volume fraction, V_f. The creep strength, therefore, merely becomes twice the load supported by the fibres, $\sigma_c = 2\bar{\sigma}_f V_f$. When linear variation of tensile stress in the fibre is assumed, the average stress $\bar{\sigma}_f$ is given by $\bar{\sigma}_f = 1/2\, \sigma_f$, where σ_f is the tensile stress at the fibre centre. We shall therefore assume that

$$\sigma_c = V_f \sigma_f = (1 - V_f) \sigma_m. \qquad (4)$$

2.2. The stress transfer

The geometry and the stress system of the model composite are illustrated by Fig. 1. The two

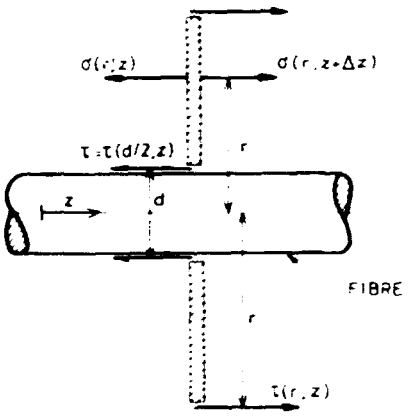

Figure 1 The stresses acting on a thin circular slice of matrix material.

hatched rectangles represent a thin circular slice of matrix. By integrating the stresses exerted on this slice we can obtain the z-component of the total force acting on it. The exact result for a single fibre embedded in the matrix is

$$2\pi r \tau = \pi d^2 \cdot 2 \int_{r_f}^{r} r' \frac{\partial \sigma}{\partial z} dr' \cdot \Delta z.$$

In a state of mechanical equilibrium the total force is zero, and in an attempt to average we shall represent the equilibrium equation of the model by

$$2\pi r \tau = \pi d^2 \cdot 2 \int_{r_f}^{r_m} r \frac{2\sigma_m}{l} dr = 0 \qquad (5)$$

We have employed Equation 3 and further set h equal to half the minimum surface-to-surface distance between fibres in the model composite. Because of the assumed hexagonal distribution, h is therefore written

$$h = \frac{d}{2}\left(\left(\frac{2\sqrt{3}}{\pi} V_f\right)^{-1/2} - 1\right) \quad (6)$$

Using Equations 4, 5, and 6 we find

$$\tau = \frac{\tau_i^* d}{2r} \quad (7)$$

where

$$\tau_i^* = \tau_i - \frac{\sigma_{0i} d}{2l}\frac{V_f}{1 - V_f}\left(\left(\frac{2\sqrt{3}}{\pi} V_f\right)^{-1/2} - 1\right). \quad (7a)$$

3. The radial velocity profile

The matrix shear stress is given by Equation 7 and the response to shear stress by Equation 1 in which $\dot{\gamma}$ is related to the relative velocity, u, between fibres and matrix through

$$\dot{\gamma} = \frac{\partial u}{\partial r}. \quad (8)$$

Using Equation 2 the rate of increase of u with increasing distance from the interface can, therefore, be written

$$\frac{\partial u}{\partial r} = \frac{3}{2}\dot{\epsilon}_0\left(\frac{\tau_i^* d}{\sigma_{0i} r}\right)^n. \quad (9)$$

By integrating $\partial u/\partial r$ with respect to r and employing the condition that there is no sliding at the interface, we find the velocity profile

$$u = u^*\left[1 - \left(\frac{2r}{d}\right)^{1-n}\right] \quad (10)$$

where

$$u^* = \frac{3}{4}\left(\frac{\dot{\epsilon}_0 d}{n-1}\right)\left(\frac{2\tau_i^*}{\sigma_0}\right)^n.$$

The reduced velocity, u/u^* is plotted as a function of r/d in Fig. 2 for a number of values of n. It is seen that the creep of the matrix is opposed only in the rather close vicinity of the fibres in the model composite, when n is not too small.

Street [9] has observed the velocity profile on the surface of a composite consisting of lead reinforced by phosphor-bronze plates. The surface was initially intersected by straight marker lines and then subjected to creep. A micrograph of the surface after creep is reproduced in Fig. 3. The straight marker lines have been deformed into curved lines giving evidence of a localized shear zone. Street [9] reports a value $n = 14$ for the lead matrix so the slope of the marker lines appears to be less than that of the velocity profiles of the model. This is undoubtedly a consequence of the idealized shear stress variation of the model, since a power relation causes the creep rate to depend quite strongly on stress. However, one might

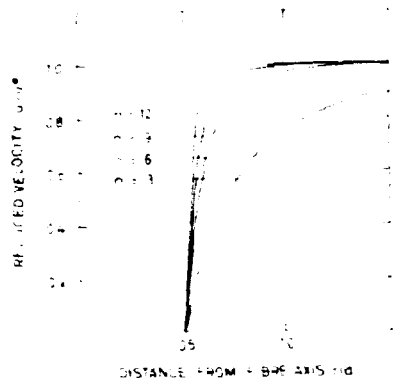

Figure 2 Profiles of reduced velocities, u/u^*, adjacent to the fibre-matrix interface, as predicted by Equation 10.

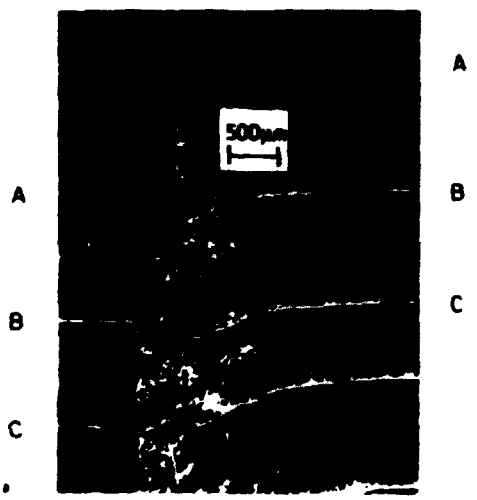

Figure 3 Optical micrograph of the tensile creep of lead embedding a noncreeping phosphor-bronze plate. The originally straight marker lines labelled A, B, C are just visible in the shear zone (Street [9]).

indeed expect the localization of shear to be less pronounced when the reinforcing members are plates rather than fibres.

4. The composite creep strength

The creep rate in the matrix was seen in the foregoing section to be disturbed only close to the fibre-matrix interface. In deducing the shear stress exerted on the interface we shall therefore disregard the presence of other fibres and employ the relationship

$$u(r, z) \to \dot{\epsilon} z \quad \text{as} \quad r \to \infty \tag{11}$$

which applies when n is greater than 1. By combining this and Equation 10 we find

$$\tau_i^* = \beta\sigma_0\left(\frac{\dot{\epsilon}}{\epsilon_0}\right)^{1/n}\left(\frac{z}{d}\right)^{1/n} \tag{12}$$

where

$$\beta = \frac{1}{2}\left(\frac{4}{3}\right)^{1/n}(n-1)^{1/n}.$$

Equation 12 has a formal similarity to Kelly and Street's result for the interface stress, but in the present case β is not a function of volume fraction.

According to assumption 2 (Section 2.1) we can express the creep strength as $\sigma_c = \sigma_f V_f$, where σ_f is determined by the force balance

$$\sigma_f = \frac{4}{d}\int_0^{L/2}\tau_i\,dz. \tag{13}$$

The interface stress is given in terms of σ_f by Equations 7a, and 12, so by substituting for τ_i in Equation 13 we find the composite creep strength

$$\sigma_c = \alpha V_f\sigma_0\left(\frac{\dot{\epsilon}}{\epsilon_0}\right)^{1/n}\rho^{1+1/n} \tag{14}$$

where

$$\alpha = \frac{(1-V_f)}{1-V_f\left(\frac{2\sqrt{3}}{\pi}V_f\right)^{1/2}}\left(\frac{2}{3}\right)^{1/n}\frac{n(n-1)^{1/n}}{n+1}.$$

In the next section it will be seen that the creep strength coefficient, α, is approximately constant.

5. Discussion and conclusions

The models developed by Mileiko, Kelly and Street, McLean, and the author all represent what might be called a perfect composite: fibres and matrix are fully adhering, the fibres are noncreeping, chemically stable, perfectly aligned, and evenly distributed. It is, therefore, interesting to compare the predictions these models give for the creep strength. It turns out that a comparison may be made very conveniently because a remarkable similarity exists between the results. By introducing the notation used in this paper and rearranging we can express the creep strength by Equation 14 for all models with expressions for the coefficients given by:

(McLean)

$$\alpha_1 = \frac{1-V_f}{V_f}\cdot 2\left(\frac{2\sqrt{3}}{\pi}V_f\right)^{1/2} - 2^{\frac{n-1}{n}}$$

(present model)

$$\alpha_2 = \frac{(1-V_f)}{1-V_f\left(\frac{2\sqrt{3}}{\pi}V_f\right)^{1/2}}\left(\frac{2}{3}\right)^{1/n}\frac{n(n-1)^{1/n}}{n+1}$$

(Kelly and Street)

$$\alpha_3 = \frac{n}{2n+1}\left[\frac{3}{2}\left(\frac{2\sqrt{3}}{\pi}V_f\right)^{1/2} - \frac{3}{2}\right]^{1/n} + (1-V_f)\rho^{\frac{n-1}{n}}$$

(Mileiko)

$$\alpha_4 = \left(\frac{n-1}{1-V_f^{(n-1)/2}}\right)^{1/n}\int_0^1 z^{1/n} + (1-z)^{1/n}\,dz$$

In McLean's coefficient, s has been replaced by $2h$ where h is given by Equation 6. The expressions for the coefficients have been computed as functions of V_f for four n-values ranging from rather small, 3 and 6, to rather greater, 9 and 12. Kelly and Street's coefficient is shown for $\rho = 50$ (dashed curve) and $\rho = \infty$ (solid curve). Although the ρ-dependence is quite significant at small V_f-values it is seen to be fairly unimportant when V_f is greater than about 20 %.

It is evident from Fig. 4 that all creep strength coefficients are nearly independent of n when $n \gtrsim 6$. The variation of α with V_f is also seen to be quite small so it seems reasonable simply to represent the coefficients by

$$\alpha_1 = 1.5$$
$$\alpha_2 = 1.2$$
$$\alpha_3 = 0.4$$
$$\alpha_4 = 0.3$$

which roughly corresponds to the α-values at

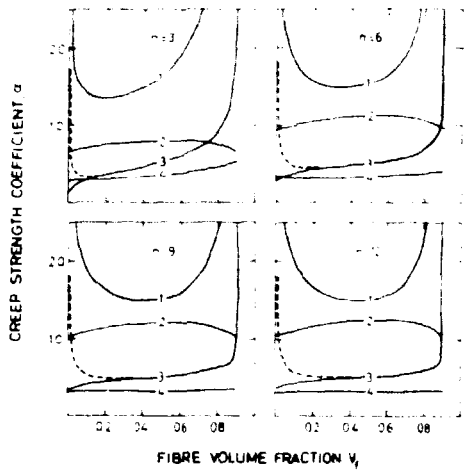

Figure 4 The creep strength coefficients, α_i. Index i refers to each curve as indicated (1, McLean, 2, present model, 3, Kelly and Street, 4, Mileiko). Kelly and Street's coefficient has been computed for $\rho = 50$ (dashed curve) and $\rho = \infty$ (solid curve).

$V_f = 50\%$ and $n = 12$. The only important point at which the four models fail to agree is therefore in predicting the creep strength coefficient. However, the predicted coefficients seem to increase with increasing assumed matrix contribution, this could explain part of the disagreement. Excellent agreement is seen between α_1 and α_3 which both take full account of the matrix and the general expression

$$\dot{\sigma}_c = \alpha V_f \sigma_0 \left(\frac{\dot{\epsilon}}{\epsilon_0}\right)^{1/n} \rho^{1+1/n}$$

where α is approximately constant and near unity seems to be very well supported by theory, since it emerges from all four treatments. Once the general expression has been experimentally verified, the decision between the various models can, therefore, be made simply by measuring the creep strength coefficient.

Acknowledgements

It is a pleasure to acknowledge the interest and encouragement of Professor R. M. J. Cotterill and Dr N. Hansen. Thanks are due to Dr H. Lilholt for helpful discussions and valuable suggestions. I particularly wish to thank Dr K. N. Street for allowing me to reproduce his unpublished micrograph here.

References

1. A. KELLY and K. N. STREET, *Proc. Roy. Soc. Lond.* **A328** (1972) 267.
2. A. KELLY and W. R. TYSON, *J. Mech. Phys. Solids* **14** (1966) 177.
3. K. N. STREET, NPL Conf., November 1971, Paper 3.
4. B. A. WILCOX and A. H. CLAUER, *Trans. Amer. Inst. Metall. Petrol Eng.* **245** (1969) 935.
5. S. T. MILEIKO, *J. Mater. Sci.* **5** (1970) 254.
6. A. KELLY and K. N. STREET, *Proc. Roy. Soc. Lond.* **A328** (1972) 283.
7. D. MCLEAN, *J. Mater. Sci.* **7** (1972) 98.
8. A. KELLY and H. LILHOLT, *Phil. Mag.* **20** (1969) 311.
9. K. N. STREET, private communication (1973).

Received 22 October and accepted 28 November 1973.

APPENDIX IV

ON A CONSTRAINT EFFECT IN STEADY STATE CREEP OF FIBRE COMPOSITES[x)]

x) Reprint of: Composites-Standards, Testing and Design. National Physical Laboratory, 8-9 April 1974. Conference Proceedings (IPC Science and Technology Press, Guildford, 1974) 33-35

On a constraint effect in steady-state creep of fibre composites

O. BØCKER PEDERSEN

The tensile creep strength of a unidirectional discontinuous fibre composite is discussed on the basis of an analysis of the equilibrium conditions in the matrix. This and previous theories predict that a volume fraction V_f of non-creeping fibres of aspect ratio l/d strengthens the matrix by the factor $\alpha\, V_f (l/d)^{1+\frac{1}{2n}}$ where n is the stress exponent in the matrix creep law. Each theory yields an approximately constant α near unity. The magnitude of α seems to reflect the importance of the constraint effect. Preliminary experimental data is presented.

1 INTRODUCTION

The fibre diameter is being recognized as an important parameter in the description of many of those properties of fibre composites that involve an interaction between the components. One of these properties is the strength under conditions of steady-state creep of a unidirectional discontinuous fibre composite containing non-creeping perfectly bonded fibres of equal length l and diameter d. As the matrix extends plastically its transverse contraction is constrained by the non-creeping fibres. This constraint gives rise to high tensile stresses in the matrix and is likely to depend upon fibre spacing, and hence upon fibre diameter for a given fibre content.

Several authors have recently analysed the steady-state creep of discontinuous fibre composites. Mileiko [1] neglects the contribution of the matrix to the load carried by the composite and Kelly and Street [2] include a contribution from an unconstrained matrix. These analyses therefore do not take the constraint effect into account. McLean [3] considers the rate of energy dissipation in the matrix during creep and derives a creep strength which is roughly three times as great as that derived by Kelly and Street. The reason for this discrepancy could be that McLean's analysis implicitly takes the constraint effect into account. We derive the creep strength by analyses [4,5] which explicitly include the full constraint effect and also by an analysis which ignores it [5]. The results of these analyses indicate that the constraint effect can amount to roughly a doubling of the composite creep strength. Preliminary experimental investigations of the Cu-W system are described and results are discussed in the light of these theories.

2 THEORY

Many metals follow a power relation between steady-state creep rate and applied stress over a fairly wide range of temperature and stress [6]. For uniaxial loading the relation takes the form

$$\sigma_{zz} = \sigma_0 \left(\frac{\dot{\epsilon}_{zz}}{\dot{\epsilon}_0} \right)^{\frac{1}{n}} \qquad (1)$$

where σ_{zz} is the tensile or compressive stress, $\dot{\epsilon}_{zz}$ is the steady-state uniaxial creep rate, and σ_0, $\dot{\epsilon}_0$, and n are constants at a given temperature. The expressions for the composite creep strength, σ_c, derived on the basis of Equation (1) by Mileiko, Kelly and Street, and McLean may all be rearranged to form the general relation

$$\sigma_c = \alpha\, V_f \left(\frac{l}{d} \right)^{1+\frac{1}{n}} \sigma_0 \left(\frac{\dot{\epsilon}}{\dot{\epsilon}_0} \right)^{\frac{1}{n}} \qquad (2)$$

in which $\dot{\epsilon}$ is the steady-state creep rate of the composite, σ_0, $\dot{\epsilon}_0$, and n are the constants appearing in Equation (1), l/d is the fibre aspect ratio, V_f is the fibre volume fraction, and α is a very slow function of V_f and n, as shown by Bøcker Pedersen [4]. At large values of n these functions are approximately given by the constant values

$\alpha_1 = 0.3$		Mileiko
$\alpha_2 = 0.5$		Kelly and Street
$\alpha_3 = 1.5$		McLean

We obtain similar results by considering the equilibrium conditions in the matrix. We select a cylindrical system of coordinates with origin, $r = z = 0$, at the fibre midpoint and z-axis parallel to the fibre axis. Assuming axial symmetry the integral form of one of the equilibrium equations is

$$2\pi r_f \tau_{rz} - \pi r_f^2 d + 2\int_{d/2}^{r} \rho \frac{\partial \sigma_{zz}}{\partial r}\, d\rho = 0 \qquad (3)$$

For large values of n the interface shear stress, τ_i, is according to several analyses [2,3,5,7,8] almost constant along the major portion of the fibre. Integration of τ_i from the fibre end therefore results in an approximately linear axial distribution of tensile stress in the fibre. A point made by McLean

Metallurgy Department, Danish Atomic Energy Commission, Research Establishment Risø, 4000 Roskilde, and the Department of Structural Properties of Materials, The Technical University of Denmark, 2800 Lyngby, Denmark

s that the tensile stress in the matrix may be calculated by a similar integration of τ_i, resulting in a nearly linear distribution of stress in the matrix, too. McLean further concludes that the load on the composite is approximately equally divided between fibres and matrix, as long as there is flow in the matrix. The large values of σ_{zz} in the matrix associated with this load distribution are possible without excessive creep-rates because the constraint generates a transverse stress, σ_{rr}, which nearly balances σ_{zz}. The corresponding triaxial stress state is described by a general relation between the stress tensor and the strain-rate tensor [9], rather than by Equation (1). However, Equation (1) does apply when the constraint effect is negligible, ie when $\sigma_{rr} \ll \sigma_{zz}$. Following these ideas we derive the composite creep strength on the basis of three different sets of assumptions.

(a) τ_i is approximately constant and any value is allowed for σ_{zz} [5].

(b) Fibres and matrix share the total load equally and the z-dependence of σ_{zz} is linear [4].

(c) The integral term in Equation (3) is negligible [5].

The first set of assumptions leads to the load distribution assumed under (b) ('equipartition of load'), which we take to represent the maximum constraint effect. Assumption (c) is taken to represent the case of no constraint effect in which σ_{zz} is given in terms of $\dot{\epsilon}_{zz}$ by Equation (1). As in previous analyses we obtain a creep strength which may be expressed by Equation (2). The appropriate a-coefficients are shown as functions of V_f for $n = 9$ in Fig. 1. The results for maximum constraint effect a_a and a_b are very similar although they are obtained by slightly different approaches. Since the dependence of a is quite small the coefficients are approximately given by the constant values

$$a_a = 1.2$$

$$a_b = 1.2$$

$$a_c = 0.5$$

The agreement between the results of Mileiko and Kelly and Street (a_1 and a_2) and a_c is fairly good as is the agreement between the result of McLean (a_3) and a_a and a_b.

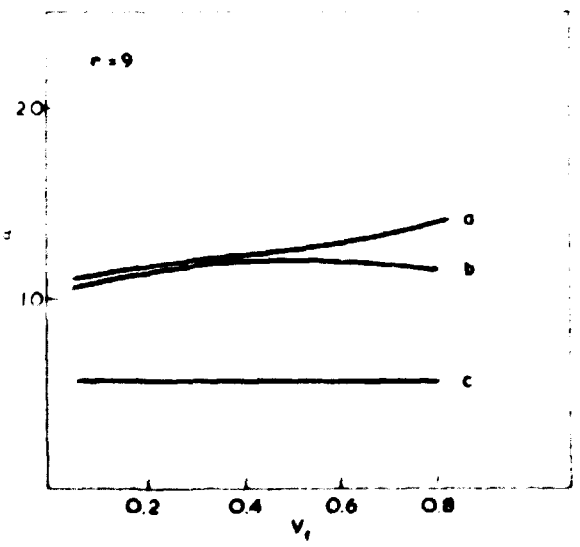

Fig. 1 Creep strength coefficients, a, derived on the basis of assumptions a, b and c

Table 1 Creep tests of discontinuous Cu-W fibre composites

Specimen	σ [MN/m^2]	$\dot{\epsilon}$ [10^{-4} h^{-1}]	A_f
1	122.6	12.59	0.22
2	103.0	20.15	0.17
2	78.5	1.89	0.17
3	103.0	1.98	0.25
4	122.6	2.78	0.22
5	137.3	13.71	0.27
5	147.2	22.27	0.27
5	157.0	44.16	0.27

The importance of the constraint effect is indicated by the difference between these two sets of results which is a factor of two or three. The constraint is likely to depend upon the mechanical properties of the components and upon geometrical factors, in particular the fibre spacing. In the region where the analyses are valid we therefore expect a_c to be a function of these variables with maximum and minimum given roughly by 1.5 and 0.5.

3 EXPERIMENTAL

The Cu-W system was investigated. Polycrystalline 0.5 mm W-wire was chopped into equal lengths and embedded by vacuum infiltration in a single crystal matrix of spectrographically pure Cu. Composite specimens of gauge length 45 mm containing a volume fraction $V_f = 0.28$ of fibres with an aspect ratio $l/d = 25$ were creep tested in air using a 13:1 lever type apparatus. Extension was magnified 200X and continuously recorded on a revolving drum. All creep tests were conducted at a temperature of 500°C ± 1°C which was measured with a thermocouple in contact with the specimen.

4 RESULTS AND DISCUSSION

Values of applied stresses and the resulting minimum creep-rates are given in Table 1 together with the fibre area fractions, A_f, observed on the rupture surfaces. The values of A_f are all less than $V_f = 0.28$ indicating, as predicted by Street [10], that rupture occurred at cross-sections of low fibre content. Fig. 1 shows a double logarithmic plot of the data in Table 1. If we disregard the measurements on specimen 2 (data points in parentheses) the plot indicates a linear relation between $\log \sigma$ and $\log \dot{\epsilon}$. The comparatively high creep rates exhibited by specimen 2 could result from the extremely low area fraction observed on this specimen, $A_f = 0.17$.

In calculating the least-squares fit represented by the line in Fig. 2 we have used only one data point per specimen (and left out the results for specimen 2), since the experimental scatter primarily results from differences in composition of the specimens. This average is appropriate when determining $\sigma_{\dot{\epsilon}_c} = \sigma_c (\dot{\epsilon}/\dot{\epsilon}_0)^{1/n}$, whereas a series of measurements on a single specimen (say those on specimen 2 or 5) appears to be more suitable when determining the composite stress exponent. The present data yield roughly the same exponent from both approaches. The creep strength determined by the least-squares method is

$$\sigma_c\ [\mathrm{MN/m^2}] = 130 \left\{ \frac{\dot{\epsilon}\ [\mathrm{h^{-1}}]}{10^{-4}} \right\}^{\frac{1}{9}} \qquad (4)$$

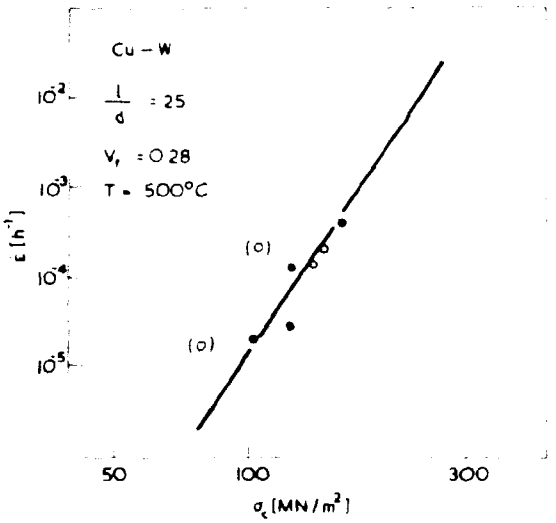

Fig. 2 Double logarithmic plot of the stresses and minimum creep rates listed in Table 1

Table 2 Matrix properties at 500°C

Reference	σ_0 [MN/m^2]	$\dot{\varepsilon}_0$ [10^{-5}h^{-1}]	n	α
11	13	10	6	0.8
12 extrapolated	25	10	5	0.4
13 extrapolated	23	10	5	0.4
14 extrapolated	16	10	5	0.6

We have not yet measured creep curves for the unreinforced matrix, but creep data on nominally pure Cu are available in the literature. Table 2 lists the parameters σ_0, $\dot{\varepsilon}_0$, and n for Cu at 500°C. Only one work [11] contains results obtained at 500°C, but the parameters were extrapolated by means of the generalized creep equation [6] from three other works [12–14]. The values of α required in order that Equation (2) predicts Equation (4) on the basis of these data are also shown in Table 2.

Experimental evidence for the constraint has usually been found in tensile experiments where the fibre spacing was considerably smaller than the average spacing $\Lambda \sim 500\mu m$ in our specimens. Kelly and Lilholt [15] observed a constraint effect for fibre spacings less than $\Lambda \sim 20\mu m$. Cheskis and Heckel [16] for $\Lambda \sim 25\mu m$, Stuhrke [17] for $\Lambda \sim 100\mu m$, and Garmong and Shepard [18] for $\Lambda \sim 2.5\mu m$. For this reason we expect the constraint effect to be fairly unimportant in the present experiments, and most of the α-values in Table 2 are indeed close to the value predicted for the case of no constraint effect. However, the unextrapolated data from the work of Pahutova et al perhaps gives the most reliable value of α, and this value is consistent with some constraint effect

ACKNOWLEDGEMENTS

It is a pleasure to acknowledge the continued interest of Professor R.M.J. Cotterill and Dr. N. Hansen. Thanks are due to Drs H. Lilholt and J.B. Bilde-Sørensen for several helpful discussions and to Messrs J. Kjøller, J. Larsen, P. Nielsen, and O. Olsen for skilful experimental assistance

REFERENCES

1 **Mileiko, S.T.** 'Steady-state creep of a composite material with short fibres', *J Mat Sci* 5 (1970) pp 254–261

2 **Kelly, A.** and **Street, K.N.** 'Creep of discontinuous fibre composites II. Theory for the steady-state', *Proc Roy Soc A* 328 (1972) pp 283–293

3 **McLean, D.** 'Viscous flow of aligned composites', *J Mat Sci* 7 (1972) pp 98–104

4 **Bøcker Pedersen, O.** 'Creep strength of discontinuous fibre composites', *J Mat Sci* (in press)

5 **Bøcker Pedersen, O.** Unpublished work

6 **Mukherjee, A.K., Bird, J.E.** and **Dorn, J.E.** 'Experimental correlations for high-temperature creep', *Trans ASM* 69 (1969) pp 155–179

7 **Kelly, A.** and **Tyson, W.R.** 'Tensile properties of fibre reinforced metals II. Creep of silver-tungsten', *J Mech Phys Solids* 14 (1966) pp 177–186

8 **de Silva, A.R.T.** 'A theoretical analysis of creep in fibre reinforced composites', *J Mech Phys Solids* 16 (1968) pp 169–186

9 **Odquist, F.K.G.** 'Multi-axial state of Stress. Mathematical theory of creep and creep rupture', *Oxford University Press* (1966) pp 19–21

10 **Street, K.N.** 'Steady-state creep of fibre-reinforced materials', *The Properties of Fibre Composites. Conference Proceedings*, National Physical Laboratory, 4 November 1971, IPC Science and Technology Press Ltd (1971)

11 **Pahutova, M., Cadek, J.** and **Rys, P.** 'High temperature creep in copper', *Phil Mag* 23 (1971) pp 509–517

12 **Feltham, P.** and **Meakin, J.D.** 'Creep in face centred cubic metals with special reference to copper', *Acta Met* 7 (1959) pp 614–627

13 **Barrett, C.R.** and **Sherby, O.D.** 'Steady-state creep characteristics of polycrystalline copper in temperature range 400°C to 900°C', *Trans AIME* 230 (1964) pp 1322–1327

14 **Monma, K., Suto, H.** and **Oikawa, H.** *J Japan Institute of Metals* 28 (1964)

15 **Kelly, A.** and **Lilholt, H.** 'Stress-strain curve of a fibre-reinforced composite', *Phil Mag* 20 (1969) pp 311–328

16 **Cheskis, H.P.** and **Heckel, R.W.** 'In situ measurements of deformation behaviour of individual phases in composites by X-ray diffraction', *ASTM STP* 438 (1968) pp 76–91

17 **Stuhrke, W.F.** 'The mechanical behaviour of aluminium-boron composite material', *ASTM STP* 438 (1968) pp 108–133

18 **Garmong, G.** and **Shepard, L.A.** 'Matrix strengthening mechanisms of an iron fiber-copper matrix composite as a function of fiber size and spacing', *Metall Trans* 2 (1971) pp 175–180

APPENDIX V

STEADY-STATE CREEP OF COPPER-TUNGSTEN FIBRE COMPOSITES*)

O. Bøcker Pedersen *)
Metallurgy Department
Danish Atomic Energy Commission
Research Establishment Risø
DK-4000 Roskilde, Denmark

Pure copper and composites consisting of aligned discontinuous tungsten fibres in a copper matrix have been creep-tested at a temperature of 500°C. The results indicate a relatively low stress sensitivity of the steady-state creep-rate for the pure copper and a relatively high stress sensitivity for the composites. This is explained on the basis of an analysis of existing creep models. A quantitative prediction of this analysis shows promising agreement with the experimental results.

*) also at:

Department of Structural Properties of Materials
Technical University of Denmark
DK-2800 Lyngby, Denmark

---

*) To be published in: Proceedings of the International Conference on Composite Materials, Geneva, 7-11 April 1975, and Boston Mass., 14-18 April 1975.

Introduction

Published theories (1-4) for the steady-state creep of composites containing aligned discontinuous fibres have only been explicitly evaluated on the basis of a power law for creep of fibres and matrix. An upsweep from a power dependence to an exponential dependence on stress is, however, commonly observed for crystalline solids (5). Bilde-Sørensen, Bøcker-Pedersen, and Lilholt (BBL) (6) have recently extended the creep models by McLean and by Kelly and Street to include the exponential creep law (or in principle any creep law) for the matrix, under conditions where the fibres do not creep. An important implication of the BBL analysis is that the upsweep to an exponential law should occur at a lower creep rate for the composite, than for the unreinforced matrix. This emphasizes the relevance of the exponential range for creep of discontinuous fibre composites.

Relatively few experiments, which could be used to check the theories, have been reported. Kelly and Tyson (7) measured the steady-state creep of discontinuous silver matrix - tungsten fibre composites under conditions where the creep of fibres was negligible. They found that there appeared to be a transition from a region at low applied stress, where $\dot{\varepsilon}_c \propto \sigma_c^3$, to a region at higher stress, where $\dot{\varepsilon}_c \propto \sigma_c^{14}$ or perhaps $\dot{\varepsilon}_c \propto \exp \sigma_c$.

The present paper describes work, which is still in progress, aimed at producing further experimental data relating to the theories. The steady-state creep of discontinuous copper-tungsten fibre composites is measured at a temperature of 500°C.

Experimental

Polycrystalline tungsten wires were obtained from Mullard Ltd., and spectrographically pure copper was supplied by Johnson, Matthey & Co. The 500 m diameter tungsten wire was given a series of equidistant notches, so that a slight bending of the wire could break it into segments of the required length. The notched wires were arranged in bundles of ten, held together by copper wire. With care, most of the notches could usually be broken by bending the entire bundle. Composite rods of diameter 3 mm were made by placing the bundle in a mould and embedding the fibres in a matrix of copper by vacuum infiltration. Specimens of gauge length L=45 mm of L=100 mm, containing a nominal fibre volume fraction V_f = 0.28 of fibres with a nominal aspect ratio of either ρ =25 or ρ =70, were made by soldering the ends of the rods into steel balls of diameter 10 mm. Specimens of pure copper were cast using the same procedure as for the composites, only excluding the fibres.

Creep tests were performed in a lever type apparatus. The extension was magnified 100X or 200X and continuously recorded. All creep tests were conducted under constant load in air. The temperature was held constant within 1°C.

Results

The composites were all creep-tested at a temperature of 500°C. No indications of oxidation of the fibres were found even after 1255 hours. Rupture always occurred within the gauge length. The creep curves normally displayed a well-developed region of steady-state creep, a few curves showed only an inversion point. Fig. 1 shows a double-logarithmic diagram of the measured steady-state creep-rates against the applied stress. Nearly all the experimental data refer to steady-state regions of duration in the range of 5 - 238 hours, a few data points (enclosed in brackets) refer to creep rates at inversion points.

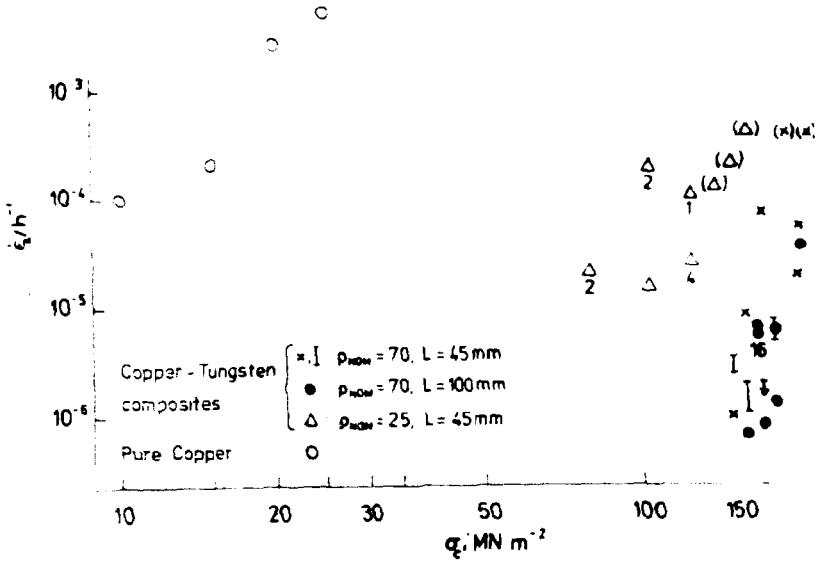

. The steady-state creep-rates of pure copper and copper-tungsten composites plotted against the applied stress. The arrow indicates a maximum point. Specimen numbers (referring to Table I) are given at some experimental points.

An increase of the nominal aspect ratio is seen to be correlated to an increase of the creep strength. The nominal fibre lengths are comparable to the gauge length L=45 mm. However, the effect of increasing the gauge length to L=100 mm appears to be fairly insignificant. Inspection of the fibres of a few specimens after dissolution of the matrix (see Table I) showed that some of the notches had not been broken. These specimens consequently contained fibres of aspect ratios which were 2, 3, or even 4 times as great as the nominal value. In some cases such a fibre actually was as long as the specimen. Further examination of the crept specimens is therefore needed, before a final interpretation of the results can be given. From the preliminary examination of the specimens listed in Table I an average aspects ratio has been calculated on the basis of the nominal aspect ratio and the number of unbroken notches. The values obtained are given in Table I and by comparing with

Fig. 1 it can be seen that an increase of the average ratio corresponds to an increase of the creep strength. Part of the scatter in fig. 1 therefore appears to result from the presence of unbroken notches.

Table I. Number of fibres, in crept composites, containing N notches

Specimen Number	Number of Notches, N				Average Aspect Ratio
	0	1	2	3	
1	30	10	2	-	32
2	28	6	-	1	30
4	23	6	2	1	34
7	21	-	-	-	70
10	19	1	-	-	73
16	17	3	3	-	98

Discussion

The few matrix points in Fig. 1 indicate a comparatively low stress sensitivity for the matrix creep, and the points for the composite indicate a rather high stress sensitivity for the composite creep. Previous predictions (1,8) of the creep strength of discontinuous fibre composites have been made from matrix creep data at the same creep-rate as measured for the composite. This implies the same stress sensitivity for the matrix and the composite. The experimentally observed stress sensitivity may, however, be understood on the basis of the BBL analysis. The essential features of

this analysis can be demonstrated by outlining the reformulation of McLean's model to comprise a general matrix creep law, rather than merely a power law.

McLean considered an aligned composite subjected to a tensile stress in the direction of the non-creeping fibres (or plates). From a geometrical argument he established the relation

$$\bar{\gamma} = \dot{\varepsilon}_c \frac{\ell}{2s} . \qquad (1)$$

He equated the rate of work done on the composite to the rate of (average) energy dissipation in the matrix, and found

$$\sigma_c \dot{\varepsilon}_c = \bar{\tau} \bar{\gamma} V_m . \qquad (2)$$

By combining eqs. 1 and 2 with a power law for creep of the matrix he finally obtained an expression for the creep strength of the composite.

In the BBL modification of McLean's approach eqs. 1 and 2 are recast as

$$\log \dot{\varepsilon}_c = \log (\tfrac{2}{3} \bar{\gamma}) + \log (\tfrac{3s}{\ell}) \qquad (3)$$

and

$$\log \sigma_c = \log (2 \bar{\tau}) + \log (\tfrac{V_m \ell}{4s}) , \qquad (4)$$

respectively. In a simple unaxial tensile creep test of the pure matrix material the conversion relations between shear values and tensile values are $\sigma = 2\tau$ and $\dot{\varepsilon} = \frac{2}{3} \dot{\gamma}$. The eqs. 3 and 4 therefore suggest that in a log $\dot{\varepsilon}_c$ versus log σ_c diagram the curve for creep of the composite may be obtained by a simple displacement of the curve for creep of the unreinforced matrix material. The displacement vector has components log $(3s/\ell)$ along the creep-rate axis and log

($V_m \ell/4s$) along the stress axis. In practice, the stress component of the displacement vector is always positive, and the creep rate component always negative ($\frac{\ell}{s} >> 1$). The transition from a power law to an exponential law should therefore occur at a lower creep-rate (and higher stress) for the composite than for the unreinforced matrix material. This provides an explanation for the high stress sensitivities observed in the experiments reported on silver-tungsten - and copper-tungsten composites.

The eqs. 3 and 4 may be expressed by a single equation

$$\sigma_c \frac{4s}{V_m \ell} = f\left(\dot{\varepsilon}_c \frac{\ell}{3s}\right) , \tag{5}$$

when the matrix creep law is introduced in the general form

$$\sigma = f(\dot{\varepsilon}) . \tag{6}$$

Similarly, the BBL analysis of Kelly and Street's model suggests the following composite creep law:

$$\sigma_c \frac{2}{\rho V_f} = f\left(\dot{\varepsilon}_c \frac{\rho}{3 e^{\frac{1}{2}\alpha}}\right) , \tag{7}$$

where α , in Kelly and Street's formulation, is given by

$$\alpha = \frac{1}{2}\left\{\left(\frac{2 (3)^{\frac{1}{2}}}{\pi} V_f\right)^{-\frac{1}{2}} - 1\right\} . \tag{8}$$

In the analysis of Kelly and Street's model it was assumed that the matrix creep law, f, could be approximated by a power law at lower stresses and by an exponential law at higher stresses.

Eq. 7 (and 5) suggests a systematic method of handling composite creep data, which in Kelly and Street's formulation implies the plotting of log ($\dot{\varepsilon}_c \rho / 3 e^{\frac{1}{2}\alpha}$) versus log ($2 \sigma_c/\rho V_f$). Such a plot has been constructed from the data in Fig. 1, using the nominal values of ρ and V_f. Within the scatter, the results for the matrix are seen to nearly coincide with those for the composites with nomi-

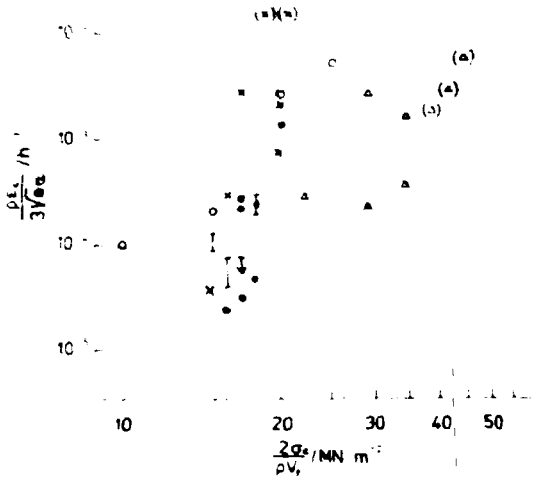

2. The experimental results from Fig. 1 replotted according to the BBL analysis (see the text for details). The symbols used for the data points are defined in Fig. 1.

nal aspect ratio $\rho_{nom} = 70$, in good agreement with the theoretical prediction. The experimental points referring to the composites with $\rho_{nom} = 25$ tend to lie to the right of the others. However, a complete examination of the actual geometry of all the crept composites is clearly needed, and this, together with the inclusion of additional experimental points, may change the picture somewhat.

Conclusions

Measurements of the steady-state creep of pure copper and discontinuous copper-tungsten fibre composites have indicated that the stress sensitivity for the composites is higher than for the pure copper at comparable creep-rates.

The experimentally observed stress sensitivity may be understood on the basis of an analysis of existing creep models.

The agreement between a quantitative prediction of this analysis and the experimental results is promising.

Nomenclature

α	geometrical parameter
$\dot{\varepsilon}$	tensile creep-rate
$\dot{\varepsilon}_c$	tensile creep-rate of composite
$\dot{\gamma}$	shear creep-rate
$\bar{\dot{\gamma}}$	average value of shear creep-rate
L	specimen gauge length
ℓ	length of fibres
ρ	aspect ratio of fibres
ρ_{nom}	nominal value of
s	spacing between fibres (or plates)
σ	tensile stress
σ_c	tensile stress applied to the composite
τ	shear stress
$\bar{\tau}$	average value of shear stress
V_f	volume fraction of fibres
V_m	volume fraction of matrix

References

1. Mileiko, S.T., "Steady-state Creep of a Composite Material with Short Fibres", Journal of Materials Science, Vol. 5, 1970, pp. 254-261.

2. McLean, D., "Viscous Flow of Aligned Composites", Journal of Materials Science, Vol. 7, 1972, pp. 98-104.

3. Kelly, A. and Street K.N., "Creep of Discontinuous Fibre Composites II. Theory for the Steady-state", Proceedings of the Royal Society, Vol. A328, 1972, pp. 283-293.

4. Bøcker Pedersen, O., "Creep Strength of Discontinuous Fibre Composites," Journal of Materials Science, Vol. 9, 1974, pp. 948-952.

5. Sherby, O.D. and Burke, P.M. "Mechanical Behaviour of Crystalline Solids at Elevated Temperature", Progress in Materials Science, Vol. 13, 1967, pp. 325-390.

6. Bilde-Sørensen, J.B., Bøcker Pedersen, O., and Lilholt, H., to be published.

7. Kelly, A., and Tyson, W.R., "Tensile Properties of Fibre Reinforced Metals II. Creep of Silver-tungsten," Journal of the Mechanics and Physics of Solids, Vol. 14, 1966, pp.177-186.

8. Street, K.N., "Steady-state Creep of Fibre-reinforced Materials", Proceedings of the Conference on The Properties of Fibre Composites, National Physical Laboratory, 4 November 1971, IPC Science and Technology Press Ltd., 1971, pp. 36-46.